UNIVERSITY OF CALIFORNIA
RIVERSIDE

Optimal Task Allocation in Crowdsourcing for Human Robot Interaction

A Thesis submitted in partial satisfaction
of the requirements for the degree of

Master of Science

in

Mechanical Engineering

by

John Hoang Duy Tran

August 2014

Thesis Committee:

Dr. Fabio Pasqualetti, Chairperson
Dr. Lorenzo Mangolini
Dr. Masaru Rao

The Thesis of John Hoang Duy Tran is approved:

Committee Chairperson

University of California, Riverside

Acknowledgments

I would like to thank my advisor, Dr. Fabio Pasqualetti, for inspiring and encouraging me to study such a challenging, but rewarding field. Taking me in as a second and last year Master's student placed a great deal of stress on him. Even with deadlines coming just around the corner, he still managed to keep his composure and professionalism as he guided me through the process of learning control theory as well as developing a thesis topic. With his support, I have learned a great deal in a very small window of time. I feel that this short-lived experience has been invaluable and something that I will remember forever. Once again, I thank Dr. Fabio Pasqualetti for putting the time and effort to my success.

To my parents, family, and friends for their constant support.

ABSTRACT OF THE THESIS

Optimal Task Allocation in Crowdsourcing for Human Robot Interaction

by

John Hoang Duy Tran

Master of Science, Graduate Program in Mechanical Engineering
University of California, Riverside, August 2014
Dr. Fabio Pasqualetti, Chairperson

Crowdsourcing is an emerging method for efficient task distribution and completion. With multiple tasks at hand, it is considerably faster to divide these tasks to multiple operators than to queue them all onto one person. A single human agent can arguably only finish one problem at any single point in time, assuming the tasks do not overlap in their description. This method is useful for real-world applications as many complex systems with a variety of tasks could be solved more efficiently. Due to pulling agents from a randomized crowd; however, we are faced with the problem of the quality of the work of each agent utilized. Efficiency will always go up the more tasks we distribute to a random crowd, but the performance or success rate may go down depending on the quality of the crowd. We then consider the question, how do we optimize various users from a crowd? In this paper, we focus on a single exogenous human factor, fatigue, and the expertise of the agents to approximate the probability of an erroneous decision from the agents. We study various fatigue models, using the Three-Process Model to compare with our model. We will also present a simplified model to predict fatigue and approximate our agents' performance due to task load and compare with current models. Considering these fatigue models, performance values of agents will be calcu-

lated to maximize our success rate depending on their task allocation. The expertise of these agents are also important in analyzing the quality of their work. We model the expertise coefficient of our agents in two fashions: a single constant value throughout the system and a dynamic value based on the drift diffusion model in optimal decision making. The studies regarding a dynamic expertise coefficient are to be completed in detail during future works. We then provide an optimal control approach using dynamic linear systems. Our model is optimized by Pontryagin's Maximum Principle from optimal control theory, allowing for analysis as a continuous function. In this thesis, the models of study are also extended into the discrete time model where we provide a new optimal policy. At the end of our thesis, we will provide an analysis of our performance model and present its success rate due to optimal task allocation.

Contents

List of Figures

Chapter 1

Introduction

Crowdsourcing is a method that allows tasks to be completed efficiently at lower costs. This is utilized when a substantial amount of tasks or data is worked with. Intuitively, a single user would take much longer than a group of users to complete a large set of tasks despite their levels of knowledge. The ability to split tasks throughout a crowd will allow for quicker completion time.

The caveat of using a crowd lies in the variance of each users' quality. A completed task does not correlate with accuracy. Accordingly, it is intuitive to say the time necessary to complete a task and the accuracy in which the task is completed is directly proportional. That is, as the performance desired increases, the time needed for completion increases.

Even with this condition, the idea of crowdsourcing is desirable in many fields, such as human robot interaction. This is due to the fact that the system will no longer require one "master" user to constantly monitor the system. This constant monitoring requires an extensive amount of time for a knowledgeable user to complete trivial assignments.

With this in mind, this thesis presents a framework to effectively use crowds at a desired performance level. The system in study is represented with a feedback control loop. The robot or controller will optimize its selection of users and distribute tasks in order to maximize its overall performance. The selection process will be highly dependent on the current performance of the user, all of which is dependent on the selection itself. The constant optimization of this cycle will lead to a maximum overall performance.

Accordingly, the controller will continue to update its selection of users as their individual performances evolve over time. This cycle is presented in Fig. 1.1, as shown.

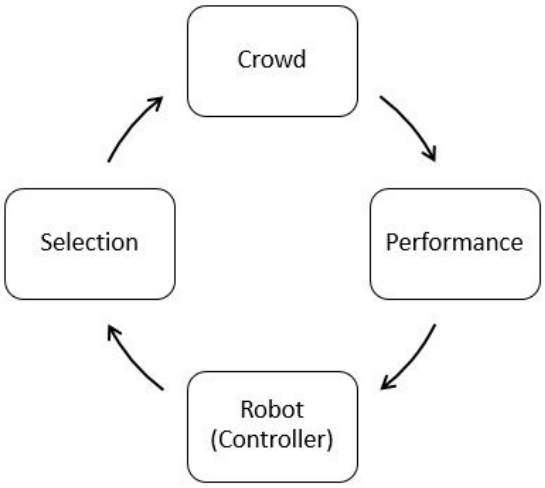

Figure 1.1: The cycle shown in Fig. 1.1 illustrates the feedback loop for the robot/controller to continue optimizing its selection of users in order to maximize performance.

Current crowdsourcing articles develop algorithms to predict the quality of each label or user through the use of priors. A prior, or prior belief, is a label that determines an individual's likelihood to make a certain decision. Ihler et al. utilizes algorithms that carefully selects priors in order to increase the performance of their system. [16] The studies completed by Ihler et al.; however, are applied for variational inference and use crowdsourcing itself as a methodology. The focus of this thesis is to create a policy in

order to effectively use crowdsourcing for such applications. The approach this thesis takes evaluates the performance of each user to be related with their respective fatigue and expertise. With that knowledge, the controller will implement a task allocation policy for performance optimization.

This thesis will discuss various models of study to consider for both the fatigue and the expertise of each user. An analytical fatigue model will be presented and compared with a current fatigue model from literature. Furthermore, the performances of the corresponding users will be extracted from their fatigue and expertise levels. This thesis will study various cases for analysis and comparison in order to develop a mathematical framework for the system. An optimal task allocation policy will be developed and implemented for each case. Preliminary findings will be discussed and illustrated prior to the conclusion of this thesis. Any future work will be described after the body of the research.

1.1 Literature Review

In this section of the chapter, the literature review completed in the field of human performance and optimal control theory will be discussed. This literature review will provide us with a body of knowledge to move forward in this thesis.

The human body is incredibly complex with countless factors affecting our "performance". The main focus of this thesis is the prominent exogenous factor that affects human performance: fatigue. Human fatigue is considerably powerful in affecting the ability to make decisions.

There are seven major biomathematical models of human fatigue that have been thoroughly studied. These models are the two-process model, the sleep/wake pre-

dictor model (Three-Process Model), the SAFE model, the interactive neurobehavioral model, the SAFTE model, the FAID model, and the CAS model [19]. This thesis will focus on the Three-Process Model for model comparison purposes.

The Three-Process Model by Åkerstedt and Folkard [23], discusses a mathematical model for approximating fatigue based on three biological systems. The respective study considers sleep cycles and time of day (sleep/wake patterns), which displays an exponential relationship. It is a complex, but effective model. It is an extended model of Peter Achermann's Two-Process Model [19] and utilizes three processes: Process C that is affected by the circadian cycle, Process S that is the exponential function from time awake to time rest, and Process S', the recovery curve that occurs during rest.

Before the details of each process are studied, assumptions to develop the model must be examined. In this model, the main change of fatigue is caused by the circadian rhythm, or the internal intrinsic clock in humans. This internal clock does not run on a perfect 24 hour day. Humans must synchronize their internal clock by exposing themselves to environmental cues, or zeitgebers, that describe the general time of the day. These cues include sunlight for the solar light cycle and moonlight for the dark cycle [10, 28]. It is instinctive to correlate night time with the "dark" half of the full cycle. This illustrates the idea that with no circadian cycle, irregular work hours would be more feasible [24]. Assuming the users that we pull from a crowd are gathered from the same time zone, then the effect from the circadian cycle is constant due to no variance between users during work hours.

The next two processes that Åkerstedt considers, deal with the sleep/wake cycle. The fatigue/alertness of a user will fluctuate depending on the amount of hours they give to each cycle. The user's alertness will asymptotically decrease as the wake cycle progresses and then increase when the user enters the sleep cycle. This model

is parallel with the idea that as a user gains a workload, their alertness will decrease due to fatigue and then increase again when they have no work to complete. Åkerstedt considers alertness for their measurement rather than fatigue. Assuming that fatigue is physically the inverse of alertness, we obtain a comparison between the proposed model and the Three-Process Model. This comparison will be illustrated in Chapter 3.

We proceed to discuss the study of linear systems and optimal control theory. We study dynamical linear systems to apply a mathematical model from our derivation and studies of human performance. Optimal control theory is then applied in order to select a control variable that will optimize our linear system. Classical control theory studies the linear system and analyzes through an iterative process to determine the change of state with respect to the state itself [15]. In our studies, the state will correlate with the fatigue of the users. These linear systems are analyzed with constraints to reach an optimal conclusion within those parameters. These design parameters can range from the state, costate, and control in order to achieve a specific optimal design.

In essence, we want to obtain the optimal input, in which the output is optimized. The problem set up will specify what the performance condition is for the output. Using optimization techniques, the system will either maximize or minimize as desired for the given optimal control. This thesis will focus on the study of Pontryagin's Maximum Principle, a commonly used method in optimal control theory that is utilized for the optimization of dynamical linear systems. Pontryagin developed the Maximum Principle initially to maximize these linear systems, but with time, the principle became more widely used for minimization. The proof for the principle from calculus of variations and optimal control theory is known to be extremely difficult, but the studies and applications are much easier. Derivation should only be considered for the Hamiltonian-Jacobi-Bellman equation of the principle. [17]

Studies show derivation of the principle was to improve upon the Weierstrass condition due to the Weierstrass condition having restrictions on the control variable [17, 18]. Pontryagin's Maximum Principle considered all admissible control variables that included Weierstrass's set. This allowed his principle to be extended for specific models such as the widely used "bang bang" control model, where the control switches instantaneously between extrema. This subset problem from the principle will display its utility and applicability further in this thesis.

Recall that our model for human performance considers both fatigue and user expertise. We extend our studies to model the probability in which the user will complete the task successfully. The preliminary work completed for expertise evolution, presented in this thesis, is the widely studied drift diffusion model based on the two-alternative forced choice model. This model will be used as a base for future work.

We present initial studies as an introduction to our future work discussed in conclusion of this thesis. In the two-alternative forced choice model, the user must decide between two choices based on the amount of evidence obtained during that set amount of time. The evidence accumulation process is modeled as the random walk process [2], where the path taken from one point to another is seemingly random. There are two main paradigms of study in which more in depth methods expand: the *free-response paradigm* and the *interrogation paradigm*. In these two different paradigms, the constraints are different and lead to different error rates (ER) [2]. These differences in error rates is equivalent to differences in the performance of the user. This is in agreement with performance studies in literature [30].

The *free-response paradigm* is a case where the user is allowed to make a choice within an infinite amount of time. There are no time constraints on the decision, which should allow the user to increase their accuracy at the cost of time. In this scenario, there

are thresholds that are generally assumed symmetrical: $\pm z$. These thresholds represent the amount of evidence accumulation required in order to make that respective decision. Most literature studies develop a right and wrong choice decision model where the right choice has a threshold of $+z$ and the wrong choice is $-z$. [2, 30]

In the *interrogation paradigm*, the decision-maker must make a choice within a small window of time. Due to this time constraint, the case may be seen as an optimal time scenario at the cost of performance. With this paradigm, the threshold becomes a single value equal to the value where the user starts their evidence accumulation process. The threshold is generally assumed zero and acts similar to the *free-response paradigm*. At the end of the time interval, if the evidence obtained is higher than the threshold limit, then the choice related to the higher limit (choice 1) is selected and vice versa.

Based on probability studies of decision making, we can analyze the performance of a user with respect to time according to the drift diffusion model. Utilizing this process, we can amend our expertise coefficient to become a dynamic process where the user gains experience over time if selected again.

The drift diffusion model is heavily studied with a wide range of applications. Current literature shows studies to improve reaction time in optimal decision theory [2, 25, 26, 27]. Extended applications blend into human decisions affecting human robot interaction for a mixed team model as studied [30, 31]. In this thesis, we formulate the framework to apply this model into crowdsourcing scenarios.

1.2 Thesis Contributions

The main contributions of this thesis are provided as follows: In **Chapter 2**, we present the studies for our model comparison, notation for further use, and technical

analysis as a framework for our simulation model. The main models of study and comparison are presented clearly in accordance to [2, 12, 17, 24, 30, 31] for future reference throughout the thesis. In **Chapter 3**, we introduce the model considered for our fatigue and performance. From this set of system dynamics, we are able to simulate and analyze the performance of single and multi-user systems, where we apply these simulations to both continuous and discrete time. Pontryagin's Maximum Principle is also presented as a policy to optimize one of our cases.

Chapter 2

Preliminary Concepts and Results

In this chapter of the thesis, we will discuss the analysis and modeling of human performances and linear dynamical systems. These mathematical models will be the basis of our studies and comparisons.

2.1 Human Performance and Fatigue Modeling

2.1.1 The Three-Process Model

The Three-Process Model studied by Åkerstedt and Folkard is a biomathematical model representing the wake cycle and the sleep cycle. Åkerstedt and Folkard considered the correspondence of alertness as an exponential function. It is discussed by Hursh et al. that most biomathematical models are approximations of a more complex biological cycle [12]. Various studies show differences in their respective models; however, common literature obtained data from mutual biological cycles. These differences in modeling alertness and fatigue curves range from linear with Hursh et al., exponential

with Åkerstedt and Folkard, and sigmoidal with Jewett and Kronauer [12, 14, 23].

Let the three processes represent alertness levels that are contingent on the time of day. The first cycle, the circadian rhythm, is presented in Process C, which is the sleepiness produced by an intrinsic biological cycle. This curve alone is only represented as a sinusoidal wave dependent on the time of the day [24]. The corresponding curve C is defined as follows:

$$C = M \cos(t - p)\frac{\pi}{12}, \tag{2.1}$$

where M is the amplitude (default = 2.5), p is the acrophase [decimal hours], and t is the time of the day [decimal hours] [23]. The peak is assumed in the afternoon with the trough in the early morning. Various studies display that the circadian rhythm is a more complex multi-oscillator cycle, rather than a simple single sinusoidal wave. Studies show that there exists secondary extrema within the main sinusoidal function [10, 11, 12, 20].

The next process is the wake cycle, modeled by the exponential S curve. The function is inversely proportional with time: as the user stays awake, the alertness will go down. This is intuitive as fatigue increases naturally over large time intervals. To oppose this reduction of alertness, a user must rest. The sleep cycle will reverse the loss of alertness exponentially as illustrated by process S' [23, 24]. The S and S' curve are as follows [24]:

$$S = [(Sa - L)e^{-0.0353t} + L] \tag{2.2}$$

$$S' = U - (U - Sr)e^{-0.381t} \tag{2.3}$$

where Sa is the value of S at an agent's awakening, L is the lower asymptote for the wake function, t is the time since awakening of the agent, Sr is the value of S at resting, and U is the upper asymptote value for the sleep/wake cycle. The function of S is measured on the alertness scale from extremely fatigued to extremely alert. These values according

to Åkerstedt and Folkard can range from 3 to 14 (with minor deviations) [23].

Literature discusses one more variable to consider: sleep inertia. Sleep inertia is the process in which a user gradually approaches maximum alertness upon entering the wake cycle. The time interval for this cycle is approximated at about two hours; however, our simulations assume users are not being selected immediately upon waking up. Let this assumption allow for the disregard of sleep inertia [22].

2.1.2 Drift Diffusion Model

To extend our expertise coefficient in our performance model, we study the in depth drift diffusion model. We utilized the drift diffusion model in order to present a dynamic expertise coefficient, where the coefficient will evolve with time for each agent. We will display preliminary studies in this thesis with areas for future research in mind.

The drift diffusion model, as stated in Section 1.1, is based off the two alternative forced choice scenario. The pure drift diffusion model is presented in the following format:

$$dx = Adt + cdW, \quad x(0) = 0, \tag{2.4}$$

where dx is the change of evidence gained over a small given time interval, dt, $A : A \to \mathbb{R}$ is the constant drift coefficient, and c is the white noise coefficient [2, 7, 25, 26].

The drift diffusion model equation has two competing factors as displayed in equation (2.4). These two parts are the constant drift, Adt, and white noise, cdW. The constant drift is considered the average gain in evidence, or "drift", towards a choice, per time unit [2]. We can analyze two different values for A according to Eckoff et al. When A is positive, the desired choice is the first one. Likewise, when A is negative, the desired selection is the second choice [7]. This model may extend these values as needed.

The white noise term, cdW, is a Gaussian distributed curve with mean 0, and variance, c^2dt [2]. We can model the performance function of the agent in question through use of the error rate in the drift diffusion model. The error rate is determined differently according to each paradigm discussed in Section 1.1. The error rates are dependent on the drift constant A, white noise coefficient c, and the threshold for making a choice $\pm z$ if *free-response* is considered.

The error rate for the *free-response paradigm* is given as

$$ER_{\text{free-response}} = \frac{1}{1 + e^{2Az/c^2}}, \tag{2.5}$$

where we assume the error is selecting the second choice. Subsequently, we can obtain the performance function of an agent by taking the complement of the error rate. That is,

$$P_{\text{free-response}} = 1 - \frac{1}{1 + e^{2Az/c^2}}. \tag{2.6}$$

The performance function is equivalent to the probability that the agent selects the first choice [2]. Making the first choice the desired answer for task completion, we can observe the performance as the expertise coefficient of each agent; however, this is for the *free-response paradigm* where the agent is allowed as much time as needed to make a selection. Our need lies in finishing the task within time constraints. With that in mind, we look to the *interrogation paradigm.*

The *interrogation paradigm* is a scenario in which the agent must make a choice in the allotted amount of time, depending on the evidence accrued as stated in Section 1.1. Recall that the selection of a choice is dependent on the evidence level at time T with respect to the threshold z. The optimal selection for the threshold is at $z = 1$, which will reduce the total error probability of the function [21]. As stated earlier, this paradigm has a different error rate as opposed to equation (2.5). The error rate for the

interrogation paradigm is given by,

$$ER_{\text{interrogation}} = \Phi\left(-\frac{A}{c}\sqrt{T}\right), \tag{2.7}$$

where $T : T \to \mathbb{R}_{\geq 0}$ is the time at the end of the decision interval and Φ is the normal standard cumulative distribution function [2, 31]. The normal cumulative distribution function is defined as follows [2]:

$$\Phi(x) = \int_{-\infty}^{x} \frac{1}{\sqrt{2\pi}} e^{-(u^2/2)} du. \tag{2.8}$$

The error rate in equation (2.7) is given as the probability that the evidence at time T is below $x(T)$ from equation (2.4) [2]. Given that we want our user to select choice 1, we can again write our performance function as

$$P_{\text{interrogation}} = 1 - \Phi\left(-\frac{A}{c}\sqrt{T}\right), \tag{2.9}$$

where our performance is dependent on the initial model conditions, A, c, and final time T. In equation (2.9), we contain no comparison values between agents for performance variability; therefore, we examine a prior probability related to each agent, in which the agent will select choice 1 [31]. We denote this prior probability as π and it affects the initial condition as follows:

$$x_0 = c^2 \log(\pi/(1-\pi))/2A, \tag{2.10}$$

where $x_0 \in \mathbb{R}$ is the initial evidence and $\pi : \mathbb{R}_{\geq 0} \times [0, 1] \to [0, 1)$ is the prior probability that the first choice is true [31]. Each agent, similar to their expertise coefficient, will have various prior probabilities for their decision making. Our new performance function with this initial condition is given by,

$$P_{\text{interrogation}} = 1 - \Phi\left(-\frac{AT - x_0}{c\sqrt{T}}\right), \tag{2.11}$$

where x_0 is equation (2.10). We plot the probability function as our performance for various prior probability values as shown in Fig. 2.1.

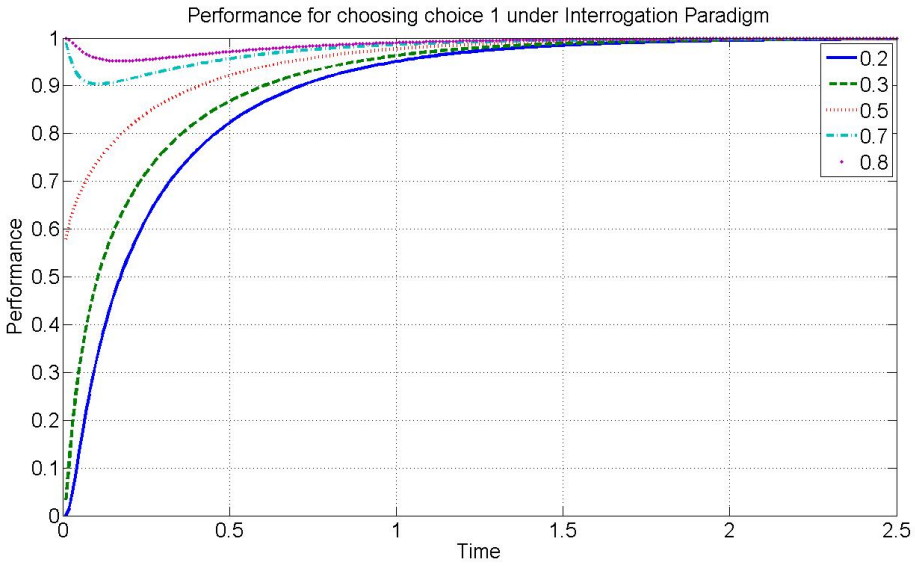

Figure 2.1: In this plot, we illustrate the various performance functions from the drift diffusion model under the *interrogation paradigm* as prior probability values, π, change.

Along with the performance curve, we present a simulation of the pure drift diffusion model with constant drift. We assume a constant drift of $A = 1$ and a constant noise coefficient of $c = 1$. Consider our initial point at $x_0 = 0$ for each trial. We obtain the "random walk model" as our evidence accumulates towards a choice with the effect of noise. At the end of our time interval, ($t = 2.5$ seconds), our trial must make a selection. The selections are shown as 3 trials for choice 1 and 2 trials for choice 2 as displayed in Fig. 2.2.

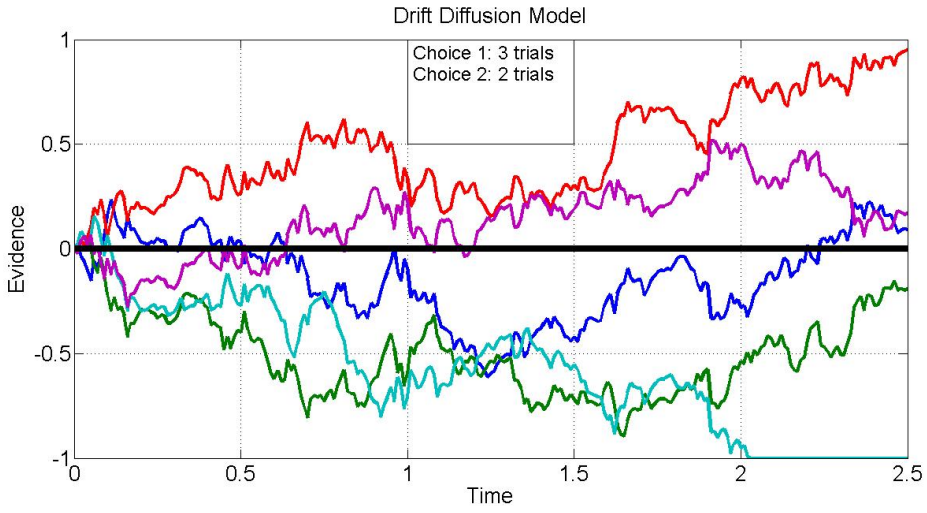

Figure 2.2: This simulation for pure drift diffusion considers a constant drift with all trials having the initial condition of $x_0 = 0$. The plot displays the model given in equation (2.4)

We assess an extension of our model into a time dependent system, we add an extra term as given in the Ornstein-Uhlenbeck (O-U) Model [2, 4, 7]. The O-U Model extends equation (2.4) as follows:

$$dx = (\lambda x + A)dt + cdW, \tag{2.12}$$

where λ is considered the reward, where x can drift towards a threshold depending on λ [2, 7]. The error rate for the O-U Model is given as

$$ER_{\text{O-U}}(T) = \Phi\left(-\frac{A}{c}\sqrt{\frac{2(e^{\lambda T}-1)}{\lambda(e^{\lambda T}+1)}}\right), \tag{2.13}$$

where $\lambda : \lambda \to \mathbb{R}$ is the additional parameter that determines the direction of rate, dx [2, 3]. Again, with this time dependent error rate, we can consider the performance as the complement of equation (2.13).

$$P_{\text{O-U}}(T) = 1 - \Phi\left(-\frac{A}{c}\sqrt{\frac{2(e^{\lambda T}-1)}{\lambda(e^{\lambda T}+1)}}\right), \tag{2.14}$$

Let this performance function be the time dependent expertise coefficient of our agent. The expertise of our agents will now begin as equality, but different agents will display

rapid growth with time to have higher expertise. This relationship is illustrated in Fig. 2.3 as various values for λ are simulated. In addition, the simulation for the O-U drift diffusion model is presented in 2.4.

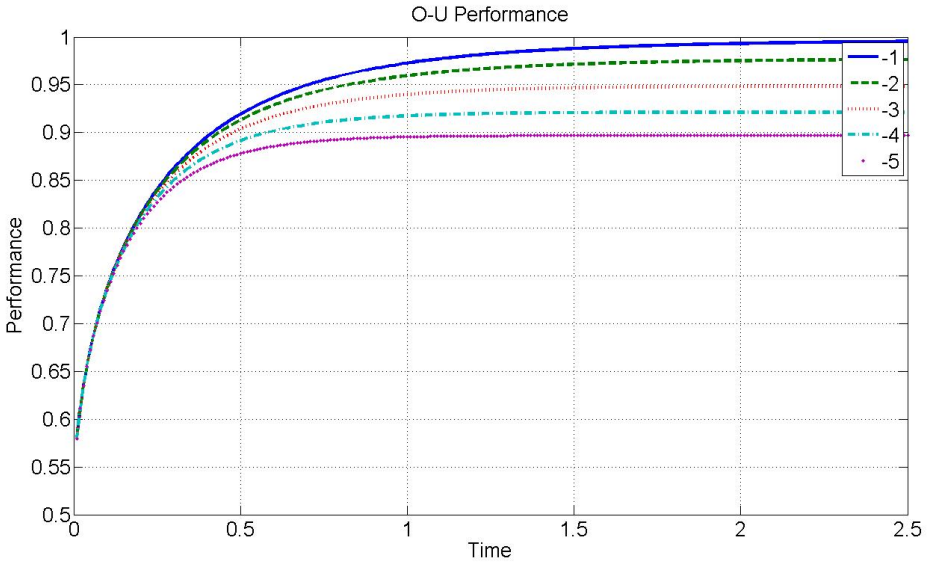

Figure 2.3: In this simulation, we display the effects of various values of λ from -1 to -5 on the performance function or the probability that the first choice is selected. This simulation is applied using the O-U Model under the *interrogation paradigm*.

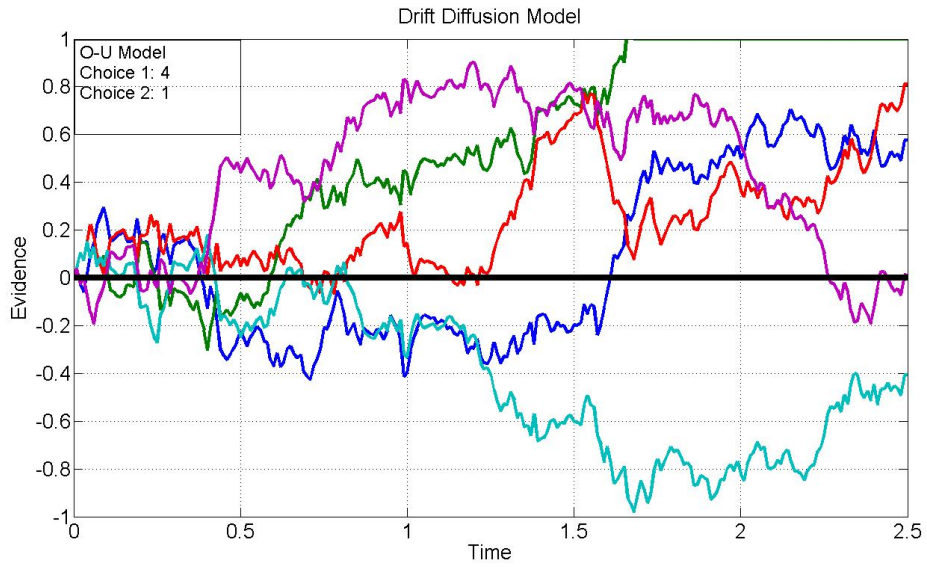

Figure 2.4: This figure illustrates the drift diffusion model under the O-U extension in which the drift rate evolves over time as shown in equation (2.12).

As an agent's probability of selecting choice one increases, their expertise coefficient increases along with it. Thus, leading to a higher individual performance value according to our model presented in Section 4.2. That model that will be presented is the preliminary work for further research and an extension of the main model.

2.2 Optimal Control Theory for Dynamical Systems

In this section, we discuss definitions and notations relevant to optimal control theory. This section will be the basis for our technical analysis and simulations provided in Section 3.

2.2.1 Dynamic Linear Systems

In this section of the thesis, we will recall the setup of optimal control theory. Our studies revolve around the dynamic linear system, which contain the state and control equation. Using this system, we may model a myriad of processes. In this thesis, we will model the dynamics of human fatigue.

Let $\mathbb{R}_{\geq 0}$ be considered a set of non-negative real numbers. To begin our model, we present the state variable, which is the core of our dynamic linear system and is given by,

$$x_i(t) \text{ for } i = [1, ..., n],$$

for $x : \mathbb{R}_{\geq 0} \to \mathbb{R}^n$, being the state at time $t \in [0, t_f]$, where $i \in \mathbb{N}$ considers multiple states.

We have a controller that we must select given by,

$$u_i(t) \text{ for } i = [1, ..., n],$$

where $u : \mathbb{R}_{\geq 0} \to \mathbb{R}^m$ is the control at time t, for each corresponding i.

Let these functions be our state and control. Here we consider our linear system to be the change of state as follows:

$$\dot{x}_i(t) = Ax_i(t) + Bu_i(t), \tag{2.15}$$

where (2.15) is a linear, continuous time-invariant system. Due to time invariance, matrix A and B are constant.

Given (2.15), we can now analyze an optimization problem for our linear system. With our state trajectory, we must select a control in order to optimize the objective or cost function of our system. Let the cost function be given by,

$$J = \phi(x_f, t_f) + \int_{t_0}^{t_f} L(x, u, t)dt, \tag{2.16}$$

subject to system dynamics and initial condition:

$$\dot{x}_i(t) = f_i(x, u, t)$$

$$x_i(t_0) = x_{i,0}$$

where $\phi \in \mathbb{R}$ considers the final state, $L \in \mathbb{R}$ relates with our Hamiltonian for optimization, and our initial condition $x_{i,0} \in \mathbb{R}$ is assumed to be at 0. The objective function, J, is the core for general optimization models considering control theory [15, 17]. We have t_0 and t_f as our initial and final time respectively, with final time being assumed "free," or not fixed at a value, for our problem statement. In order to optimize our model, we follow the studies of Pontryagin's Minimum Principle as discussed in Chapter 2.2.2 of this thesis.

2.2.2 Pontryagin's Maximum Principle

Consider the objective function and the system dynamics from equation (2.16). We want to find an admissible control, u^*, where

$$u \in U$$

is the set of admissible controls, such that our system

$$\dot{x}_i(t) = Ax_i(t) + Bu_i(t)$$

follows its admissible state trajectory, x^*, so that equation (2.16) is optimized. [15, 17]

Considering that J is maximized (or minimized), we obtain u^* and x^* as our "optimal" control and state trajectory as desired. Obtaining these optimal trajectories is the goal of Pontryagin's Minimum Principle. The proof for Pontryagin's Principle will be discussed further in this section. Pontryagin's Minimum Principle was developed as a proof that expanded on the initial Weierstrass condition's set of controls. We consider Pontryagin's Maximum Principle (the original principle), with the minimum version in mind for specific cases. The two models are parallel and are dependent on the necessity of maximizing or minimizing the cost function. Weierstrass's condition required the Hamiltonian to be minimized over the set of all admissible controls, u, where u is limited to continuously differentiable and unbounded functions. Pontryagin et al. expanded those set of controls to include all "measurable" functions [17]. The Minimum Principle states that the Hamiltonian must be minimized over the set of all admissible U. With the Maximum Principle, we state that the Hamiltonian must be maximized over the set of all admissible U. [17] This is in accordance with our statement that the two models are identical.

In short, the principle states that our cost function (2.16) is optimized if an optimal control u, with respect to the system dynamics (2.15), is selected such that the

respective Hamiltonian functions agree with the principle. This will be discussed below in detail.

Consider an optimal control problem, in which we want to maximize our objective function, J, as given in equation (2.16). Assuming from above that $u^*(t) \in U$ will force J to be maximized, we can then proceed with the optimization analysis.

The Hamiltonian can be written as

$$H(x_i, u_i, t, \lambda_i) \equiv L(x_i, u_i, t) + \lambda_i^T f_i(x_i, u_i, t) \tag{2.17}$$

where H is the Hamiltonian and λ is the costate function [15, 33].

To progress, we must consider the costate function from calculus of variations. Through our studies, we note that combining an Euler condition theorem with the *transversality condition* theorem, we can obtain the *Multiplier Rule* [8]. This rule developed by Bliss, states that continuous costate functions, $\lambda_i(t)$, on $[t_0, t_f]$ for $i = [1, ..., n]$ exists such that the following is true at each t: [8, 15]

$$\dot{\lambda}_i = -H^*_{x_i} \tag{2.18}$$

$$(i = 1, ..., n) \tag{2.19}$$

where $-H^*_{x_i}$ is the negative partial of the Hamiltonian with respect to x. This allows us to obtain our first vital equation for optimizing.

The *transversality condition* is a terminal condition on the costate variables where time, t, to reach the target is minimized. The *Multiplier Rule* given above tells us that costate functions are equivalent to the partial derivatives of the Hamiltonian. This is a necessary rule for us to proceed with the analysis.

For the assumptions given above, we obtain Pontryagin's Maximum Principle:

Condition 1. *Pontryagin's Maximum Principle*

$$H[x^*(t), u^*(t), t, \lambda(t)] \geq H[x^*(t), u(t), t, \lambda(t)] \tag{2.20}$$

where if condition 1 holds true, then the objective function (2.16) is maximized [17].

By taking the partial derivative of our Hamiltonian with different variables, we define the state and the costate equations:

$$\dot{x} = \frac{\partial H}{\partial \lambda}(x, u, \lambda) = f(x, u) \tag{2.21a}$$

$$\dot{\lambda} = -\frac{\partial H}{\partial x}(x, u, \lambda) = -\frac{\partial L}{\partial x}(x, u) - (\frac{\partial f}{\partial x}(x, u))'\lambda \tag{2.21b}$$

where $\dot{x}$ is the state equation and $\dot{\lambda}$ is the costate equation for the Hamiltonian system. Let $u(t)$ be in the domain of admissible controls with an admissible state $x(t)$ from that control. We then define a solution $\lambda(t)$ that corresponds with the Hamiltonian system. Provided these equations, we can optimize problems formulated with linear systems through the use of Pontryagin's Maximum Principle [1].

Chapter 3

Optimal Task Allocation

This chapter contains the main results of this thesis. We start by describing our models for characterizing the performance of the human user which is dependent on the fatigue level, the expertise, and the tasks to be accomplished. Then, we derive optimal policies to allocate tasks while maximizing performance.

3.1 Model of User's Fatigue

In this section we model the fatigue and the performance of a human user as a function of his/her workload over time. Intuitively, the performance of a user in inverse-proportional to his/her fatigue, while the fatigue is proportional to the workload and work time. Then, in order to optimize the performance of an user, it is necessary to modulate the workload so as to maintain the fatigue level around an optimal value. For our study we assume that the fatigue $x_i : \mathbb{R} \to \mathbb{R}$ of the user i evolves according to the linear continuous-time dynamics

$$\dot{x}_i(t) = -\alpha_i x_i(t) + u_i(t), \tag{3.1}$$

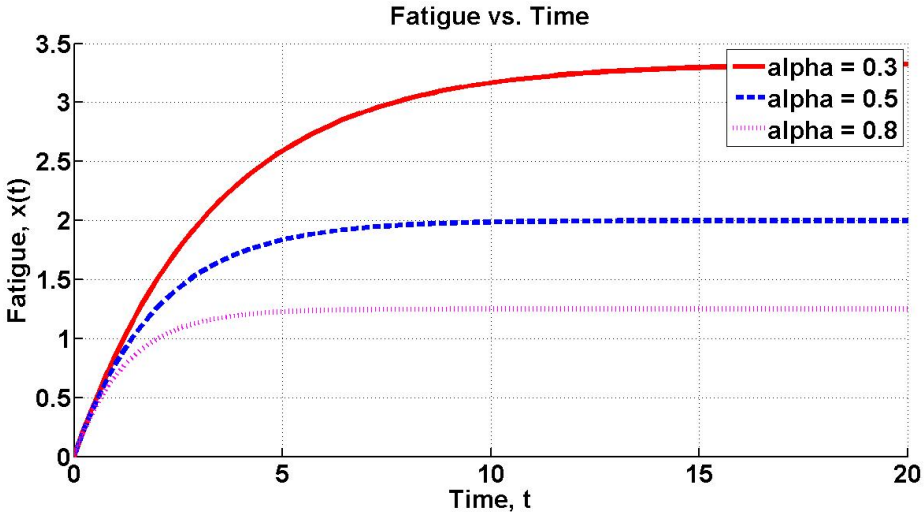

Figure 3.1: In this figure, we display the monotonically increasing exponential relationship of fatigue considering constant task load. It is observed that different values for the recovery constant provide various fatigue curves. As t approaches ∞, our maximum fatigue has a value of $\bar{u}/\alpha_i$.

where $\alpha \in \mathbb{R}_{>0}$ is the *recovery constant* of user i, and $u_i : \mathbb{R} \to \mathbb{R}$ is the workload assigned to the ith user. Without affecting generality, we assume that $x_i(0) = 0$, that is, the ith user has zero fatigue level at time $t = 0$, and $0 \leq u_i(t) \leq 1$ at all times $t \in \mathbb{R}_{\geq 0}$. The recovery constant α_i is a coefficient that relates with each individual user and quantifies various aspects such as exhaustion, lifestyle, and boredom.

It should be observed that, as the task load increases, it begins to compete with the negatively exponential value of the fatigue, allowing for the rate of fatigue change to obtain its value depending on which factor outweighs the other. As the recovery load outweighs the task load, the rate of fatigue change becomes negative, allowing the fatigue value to decrease. When the task load outweighs the recovery load, the rate of fatigue change becomes positive, forcing the fatigue to increase. This discussion is in accordance with the intuition that the more work one user completes, the more fatigue he/she will become.

The dynamic evolution of the fatigue can be explicitly computed. In fact, from

the dynamic model (3.1) we obtain

$$x_i(t) = e^{-\alpha_i t} x_i(0) + \int_0^t e^{-\alpha_i (t-\tau)} u_i(\tau)\, d\tau. \tag{3.2}$$

When the user is assigned no load work, that is, u_i is identically zero, then $x_i(t) = e^{-\alpha_i t} x_i(0)$, which shows the exponential recovery behavior, that is, the fatigue level exponentially decreases to zero in the absence of workload. Instead, when the workload is constant and equal to $\bar{u}$, we have

$$x_i(t) = e^{-\alpha_i t} x_i(0) + \frac{\bar{u}}{\alpha_i}(1 - e^{-\alpha_i t})$$

The evolution of the fatigue for different recovery constants and constant load are shown in Fig. 3.1. It should be observed that the fatigue is monotonically increasing, so that the maximum fatigue level is asymptotically obtained at $t = \infty$, and it equals $\bar{u}/\alpha_i$. It is important to note that our fatigue model only depends on the workload, and it neglects other factors, such as the circadian rhythm, homeostasis, and sleep inertia. Hence, our model is most relevant when the workload has a short duration with respect to a typical work shift.

To perform a model comparison, we show that equation (3.1) is in accordance with the Three-Process Model described in Section 2.1.1. In fact, in comparison with equations (2.2) and (2.3), we observe many similarities.

We are provided the following variables and constants: Sa is assumed 14, L is given as 2.4, Sr is assumed to be 7.96, and U is the upper asymptote at 14.3 [23, 24]. These values being assumed are on the alertness scale where "7" is the sleepiness threshold, "3" is extreme sleepiness, and "14" is very little sleepiness or extremely high alertness.

For comparison purposes, we scaled down the Three-Process Model with the one we provided in equation (3.1). We assume a 24 hour period of fatigue gain and a 24

hour period of alertness gain for both models. Let alertness be represented in parallel with performance. Our model comparison is shown in Fig. 3.2.

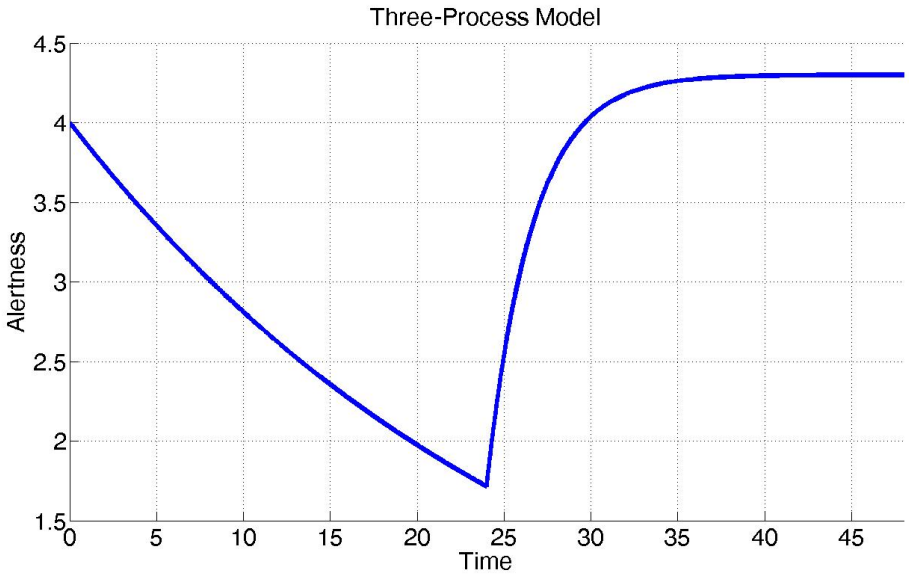

(a) Three-Process Model

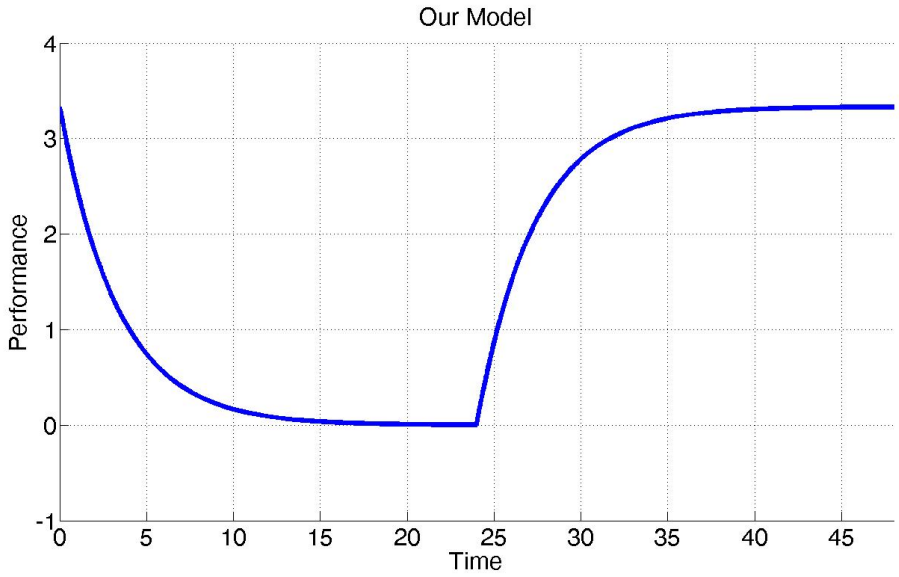

(b) Our Model

Figure 3.2: This figure illustrates the similarities between our model and the Three-Process Model developed by Åkerstedt et al. in terms of performance and alertness. There is a slight discrepancy in the time scale, but both models visually convey a similar relationship. [23]

It is important to note that we disregard the circadian process in both models.

We assume minute differences due to the circadian rhythm between users. This assumption agrees with the policy that our controller will select users in an environment where the circadian rhythm is controlled.

3.2 Model of User's Performance

In this section we characterize the performance of a human user with respect to his/her fatigue level and his/her assigned workload. We adopt the following exponential model of user's performance $P_i : \mathbb{R} \to \mathbb{R}$,

$$P_i(t) = k_i e^{-x_i(t)}, \tag{3.3}$$

where $k_i \in \mathbb{R}$ is a constant representing the expertise of user i. Notice that the performance function P_i is exponentially decreasing with the fatigue level, and that, since the fatigue level is nonnegative, its maximum value coincides with the expertise k_i. In Fig. 3.3, we show the dynamic behavior of the performance P_i when the workload is constant for different recovery and expertise constants. It illustrates the critical point at which the tradeoff between expertise and recovery occur.

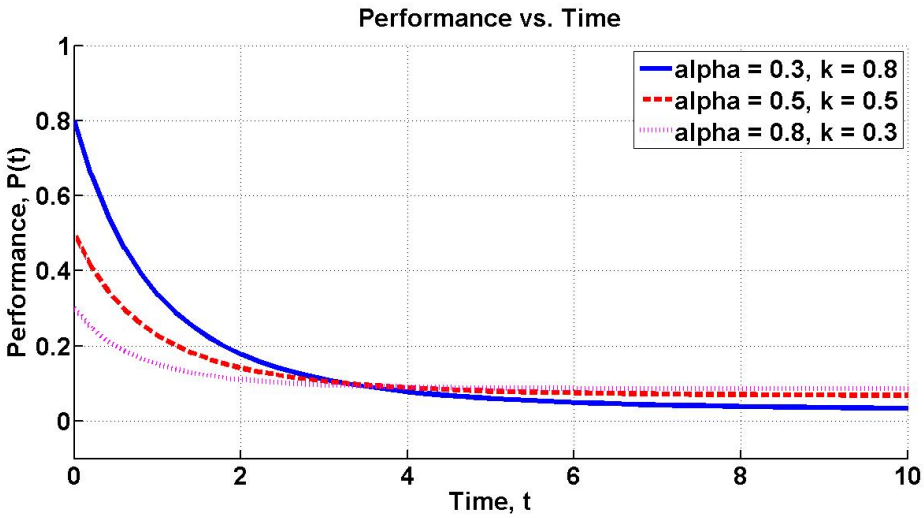

Figure 3.3: Fig. 3.3 displays the dynamic behavior of our performance curve considering various recovery and expertise coefficients for a constant workload.

Given (3.3), we analyze that the fatigue is minimum when performance is maximum and vice versa. This is in accordance with our intuition in Section 3.1 and simulations as shown in Fig. 3.3. It is also observed that the expertise coefficient will shift the entire performance with a direct relationship. It is concluded that a higher expertise coefficient will lead to higher performance as analyzed. It is important to understand this competitive feedback behavior for our optimization.

Assuming a constant recovery rate and task load with various expertise coefficients, the performance curve is observed to have a steadily decreasing exponential curve. Each curve is offset to match the expertise coefficient, where users with more expertise will output a higher performance. Consider the same scenario with different recovery rates, but constant expertise; it may be observed that the starting performance at zero fatigue will be equal for all users. The equality of their expertise provide an equal initial performance output before fatigue begins to influence the performance.

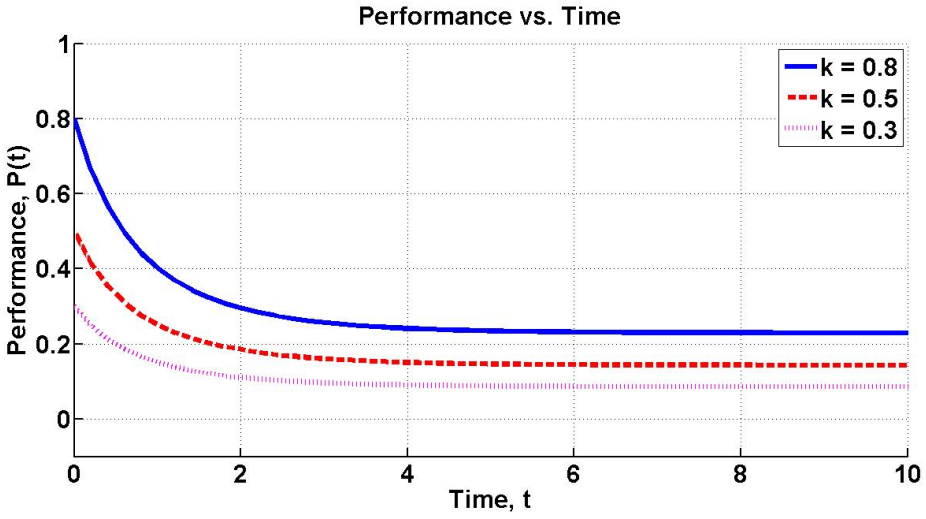

Figure 3.4: The performance curve considering different values of k_i.

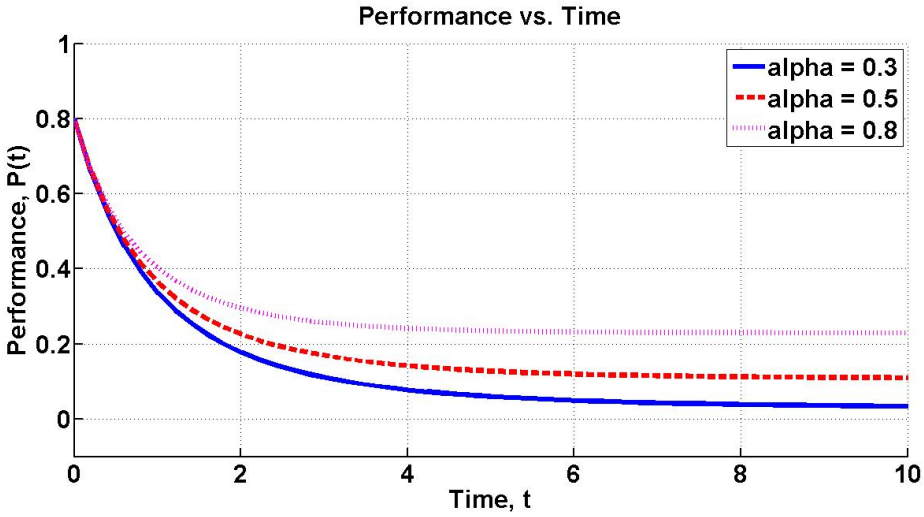

Figure 3.5: The performance curve considering different values of α_i

Given Fig. 3.4 from above, we observe the direct proportional relationship of performance with the expertise coefficient. That analysis is considering a constant expertise coefficient, k_i with equation (3.3). In terms of future work, studying a dynamic expertise coefficient must be done. Preliminary analysis will be displayed in Section 4.2.

3.3 Continuous Task Allocation for Single User

Consider the scenario in which a single user has to complete the tasks assigned by a robot. Let the fatigue level of the user be described by (3.1), and let the user performance be as in (3.3). We consider the overall performance function to be

$$J_{\text{C-S}} = \int_0^{t_f} \left(\frac{1}{\alpha} - x \right) u dt, \tag{3.4}$$

where t_f is a time horizon of interest. The cost function $J_{\text{C-S}}$ is a measure of the tasks successfully completed by the user. In fact, $u(t)$ denotes the workload assigned to the user, while $\frac{1}{\alpha} - x(t)$ measures the productivity of the user at time t, since $x(t)$ is the fatigue level at time t, and $1/\alpha$ is the maximum fatigue level due to equation (3.2). Our

objective is to design the workload $u : \mathbb{R} \to [0, 1]$ so as to maximize the cost function $J_{\text{C-S}}$.

To address our optimization problem we resort to *Pontryagin's Maximum Principle*; see Chapter 2. For the dynamics (3.1) and the objective (3.4), the Hamiltonian function is found to be

$$H = \left(\frac{1}{\alpha} - x\right) u + \lambda \left(-\alpha x + u\right), \tag{3.5}$$

where λ is a vector of Lagrange multipliers. In the absence of constraints on the workload, the optimal workload profile and the costate would satisfy

$$\frac{\partial H}{\partial u} = 0 = \frac{1}{\alpha} - x + \lambda, \;\; \Rightarrow \;\; \lambda = x - \frac{1}{\alpha}.$$

Taking the negative partial derivative of equation (3.5) with respect to x, we may obtain our costate equation:

$$\dot{\lambda} = -\frac{\partial H}{\partial x} = \alpha\lambda + u.$$

By combining the above equations with the dynamics (3.1) we obtain $\dot{\lambda} = \dot{x}$, or equivalently,

$$\alpha x - 1 + u = -\alpha x + u.$$

Consequently, the optimal fatigue level is found to be

$$x^* = \frac{1}{2\alpha},$$

and the optimal workload u^* is such that it drives the fatigue level up to the optimal level x^* as fast as possible, and then maintains such value. Our discussion is summarized in the following theorem.

Theorem 2. ***(Optimal continuous task allocation for a single user)*** *Consider a single user with fatigue dynamics*

$$\dot{x} = -\alpha x + u,$$

where $\alpha \in \mathbb{R}$ *and* $x(0) = 0$. *The optimal task allocation* $u^* : \mathbb{R} \to [0, 1]$ *that maximizes the cost function*

$$J_{\text{C-S}} = \int_0^{t_f} \left(\frac{1}{\alpha} - x \right) u dt,$$

is as follows:

$$u^* = \begin{cases} 1, & \text{if } x < \frac{1}{2\alpha}, \\ 0, & \text{if } x \geq \frac{1}{2\alpha}. \end{cases}$$

In Theorem 2, we derive the continuous optimal task allocation policy for a single user. It should be observed that the optimal task allocation policy is in fact a *Bang Bang* control law, where the task allocation is either zero or maximum. This type of controller is typical in constrained optimal control applications [15].

Although optimal, the control policy u^* in Theorem 2 has some undesirable features that may limit its applicability in a practical application where there may be a limit on the switching rate between the zero and unit workloads. Limitations in the switching rate would result in oscillations in the fatigue level and performance, as shown in Fig. 3.6 and 3.7. One possible solution is to design a (suboptimal) *feedback controller* to maintain the fatigue level at its optimal value.

Theorem 3. ***(Steady state optimal controller)*** *Consider a single user with fatigue dynamics*

$$\dot{x} = -\alpha x + u,$$

where $\alpha \in \mathbb{R}$ *and* $x(0) = 0$. *The constant workload* $\bar{u} = 0.5$ *satisfies*

$$\lim_{t \to \infty} x(t) = x^* = \frac{1}{2\alpha}.$$

Proof. The statement follows directly from equation (3.2). □

The task allocation policy $\bar{u}$ described in Theorem 3 achieves a lower performance with respect to the optimal policy u^* described in Theorem 2. Yet, the policy $\bar{u}$ is asymptotically equivalent to u^*, as they both achieve the same fatigue level, and it does not depend on the maximum allowable switching rate as for the case of u^*. A comparison between the performance of $\bar{u}$ and u^* is reported in Fig. 3.7.

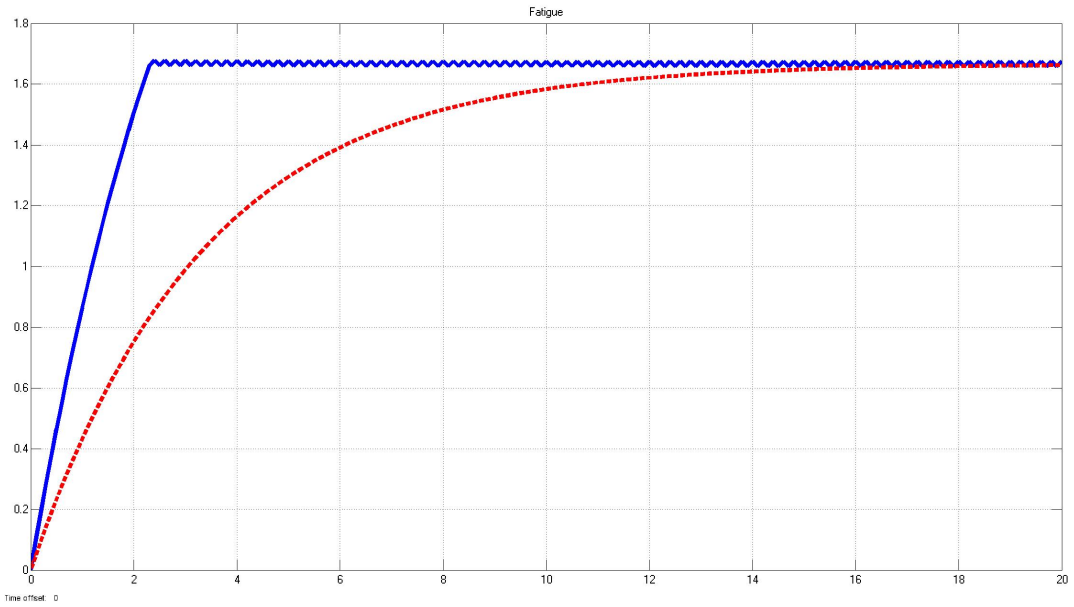

Figure 3.6: A simulation presenting the fatigue curve, illustrating the *Bang Bang* control model. Blue: Optimal conditions representing Theorem 2. Red: Steady state conditions from Theorem 3.

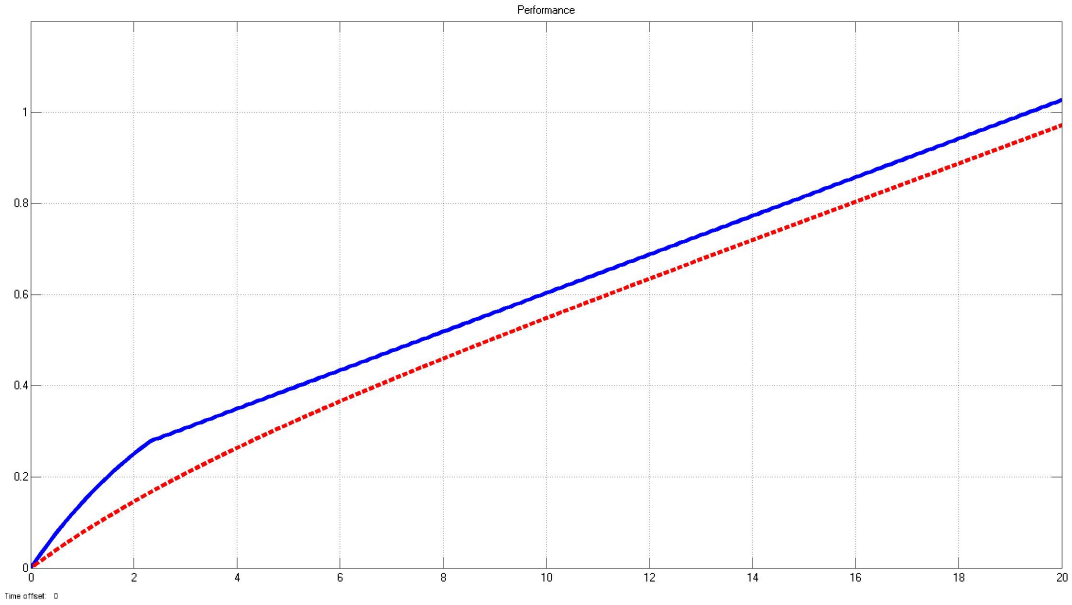

Figure 3.7: Performance curve from our *Bang Bang* control model simulation. The red and blue simulations match Fig. 3.6 respectively.

It may be noted that in the first case with the *Bang Bang* control, we have multiple continuous switches as time progresses. In the steady state policy, the user will undergo zero switches. If desired, a controller may utilize a merged policy that requires the user to experience one switch; the switch from the *Bang Bang* control policy to the steady state policy. This will allow the user to converge to the optimal fatigue level after reaching the critical point in the *Bang Bang* policy.

3.4 Continuous Task Allocation for Multiple Users

Consider the scenario in which the robot can assign the tasks to be completed to different users to optimize their overall performance. Let the fatigue level of each user be described as in (3.1), and let the performance of each user be as in (3.3). We consider the overall performance function to be

$$J_{\text{C-M}} = \frac{1}{Nt_f} \sum_{i=1}^{N} \int_0^{t_f} P_i(t) u_i(t) dt, \tag{3.6}$$

where N is the total number of users, $P_i : \mathbb{R} \to \mathbb{R}$ denotes the performance of user i, and $u_i : \mathbb{R} \to [0, 1]$ is the workload assigned to user i. For notational convenience, we assume that

$$\sum_{i=1}^{N} u_i(t) = 1, \tag{3.7}$$

at all times t.

To design an optimal task allocation, notice that each term $P_i(t)u_i(t)$ is nonzero at all times t. Moreover, due to assumption (3.7), the function

$$\sum_{i=1}^{N} P_i(t)u_i(t),$$

is a *weighted average* of the performances P_i. Hence, the cost function (3.6) is maximized by assigning the entire workload to the most performing user at each time. We summarize this discussion in the following theorem.

Theorem 4. ***(Optimal controller for multiple users in continuous time)*** *Consider N users with fatigue dynamics*

$$\dot{x}_i = -\alpha_i x_i + u_i, \ i \in \{1, \dots, N\},$$

where $\alpha_i \in \mathbb{R}$, and $x_i(0) = 0$. The task allocation $u_i^* : \mathbb{R} \to [0, 1]$, with $\sum_{i=1}^{N} u_i(t) = 1$ at all times t, that maximizes the cost function

$$J_{\text{C-M}} = \frac{1}{Nt_f} \sum_{i=1}^{N} \int_{t_0}^{t_f} P_i(t)u_i(t)dt,$$

is as follows:

$$u_i^*(t) = \begin{cases} 1, & \text{if } P_i = \max\{P_1, \dots, P_N\}, \\ 0, & \text{otherwise.} \end{cases}$$

From theorem 4 we conclude that an optimal task allocation for the cost function $J_{\text{C-M}}$ in (3.6) is so that the performance levels of all users are all equal to each other. Hence, the performance of the *crowd* is in fact dictated by the performance of each single user, and not only by most performing one. The dynamic behavior of the fatigue levels and the performances for a group of three users is reported in Fig. 3.8(a) and Fig. 3.8.

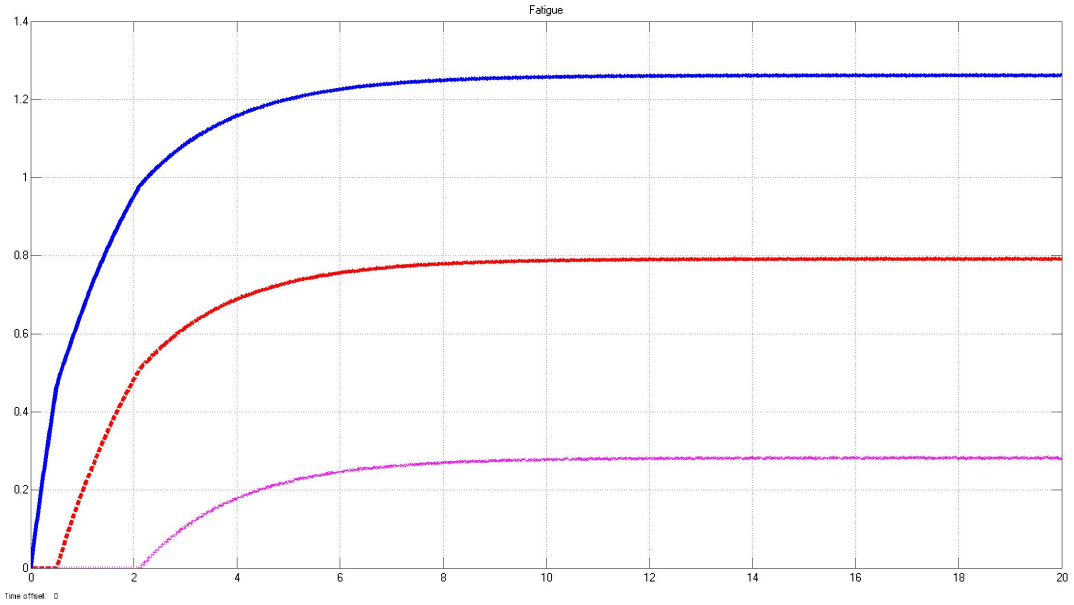

(a) The dynamic fatigue curve for 3 users undergoing full task load and rest through Pontryagin's Maximum Principle.

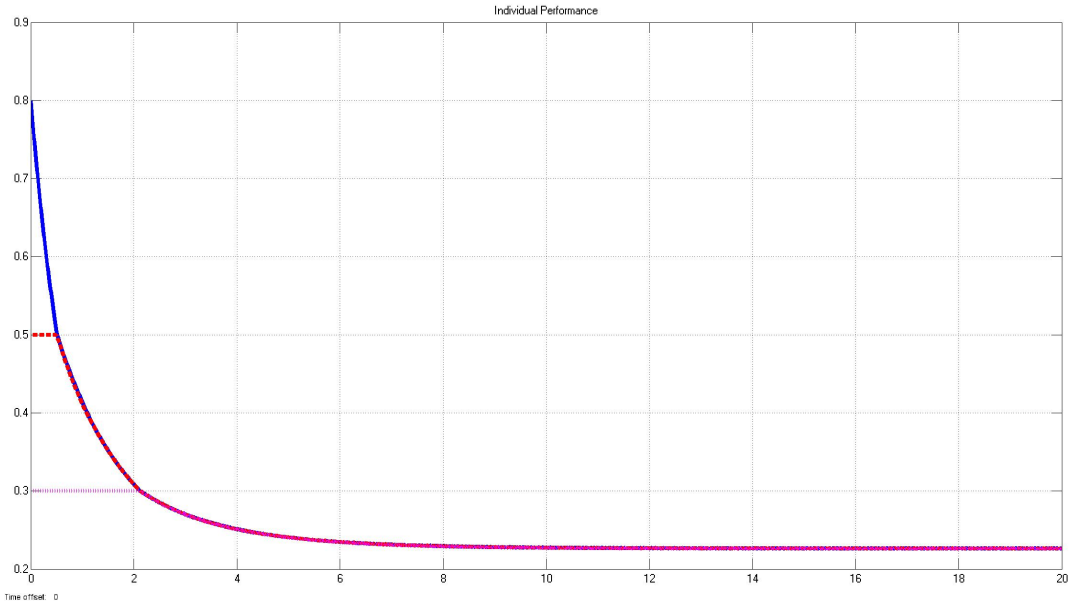

(b) Performance of the 3 users considering dynamic fatigue (recovery) and dynamic task load

Figure 3.8: In Fig. 3.8, we observe a dynamic linear system of fatigue for 3 users with various recovery and expertise coefficients. In Fig. 3.8(a), it is seen that users may fatigue and recover continuously depending on their dynamic task load. Note that as time increases, the fatigue approaches an asymptotic value which conforms with our analysis in Section 3.1. The solid, dashed, and dotted lines represent 0.3, 0.5, and 0.8 for α and 0.8, 0.5, and 0.3 for k_i respectively. In Fig. 3.8(b), we examine the respective individual performance of each user dependent on their above fatigue.

To obtain the overall performance of our model. we simulate equation (3.6) with the above data. Through this analysis, we acquire the optimum performance from the correct selection algorithm as seen in Fig. 3.9. For completeness, we compare the optimal task allocation described in Theorem 4 with other allocation policies.

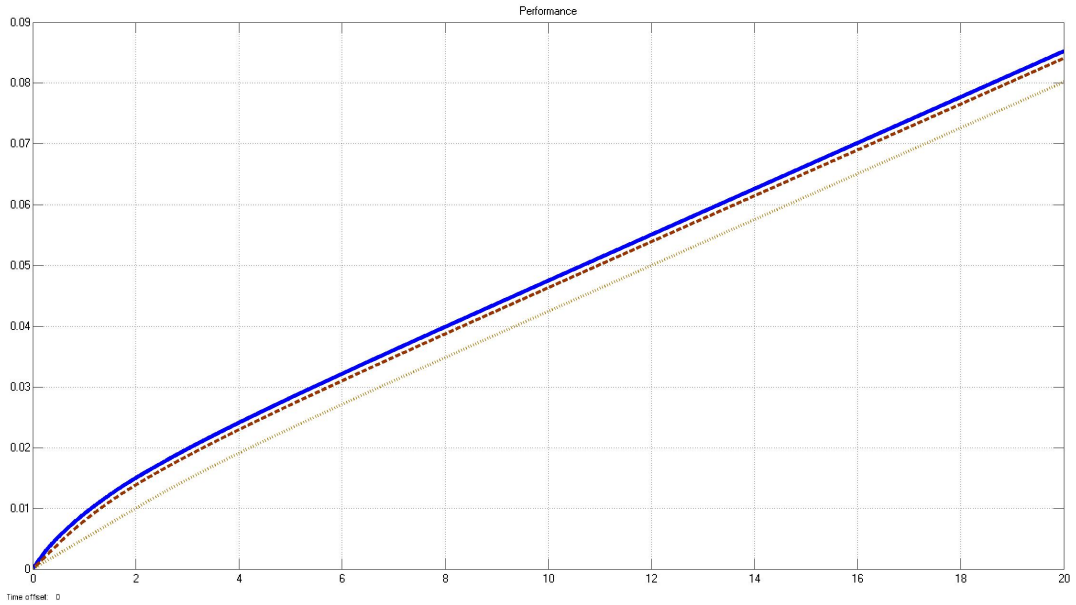

Figure 3.9: In this figure, we present the overall performance modeled from equation (3.6). Upon inspection, we note that our optimal controller produces the highest performance curve (solid-blue) in comparison with suboptimal controllers (brown and grey). This is in agreement with Theorem 4.

3.5 Discrete Task Allocation for Multiple Users

In the previous sections we have considered continuous-time models, where tasks are assigned and completed instantaneously. Instead, we now consider the case in which each task has a fixed duration so that, once assigned to user i, it must be completed by user i. In our mathematical framework, the assumption that tasks have a fixed duration is captured by considering the workload u to be piecewise constant, and that it is updated at discrete time instants.

To obtain our discrete-time dynamical model of fatigue and performance for

piecewise constant workload, we discretize (3.1) that becomes:

$$x_i(t_{k+1}) = \alpha_i^d x_i(t_k) + b_d u_i(t_k),$$

where $t_k = kT$, T is the duration of each task, and $k \in \{0, 1, \dots\}$. Moreover,

$$\alpha_i^d = e^{-\alpha_i T}, \text{ and } b_d = \frac{1}{\alpha_i}(1 - e^{-\alpha T}),$$

where α_i is the i-th recovery coefficient.

Since the workload is piecewise constant, the cost function (3.6) can be written as

$$J_{\text{D-M}} = \frac{1}{NM} \sum_{i=1}^{N} \sum_{k=1}^{M} P_i^d(t_k) u_i(t_k) T,$$

where

$$P_i^d(t_k) = k_i e^{-x_i(t_k)}.$$

This cost function is obtained from a simplification of our model. We note with this definition that $J_{\text{D-M}}$ is not the counterpart to our continuous model, $J_{\text{C-M}}$. In order for the two cost functions to be parallel, P_i^d should be analyzed as an integral; however, the analysis of this integral is nontrivial, so we save this analysis for future work.

Following our procedure in Section 3.4, the maximization of the cost function $J_{\text{D-M}}$ is obtained by assigning the whole workload to the user with largest P_i^d. However, since P_i^d depends on the user fatigue level and workload, and because users have different expertise and recovery rates, the computation of the optimal allocation policy is nontrivial.

With this in mind, we continue to propose an optimal policy for our discrete time case. Recall that each task is now considered to be piecewise constant. Our optimal policy requires the controller to consider the performance curve of each user at each time

frame, t_k. The controller will then allocate the whole workload, $u = 1$, to the current highest performing user at the beginning of each discrete time block. Each other user will be at rest until the next iteration occurs for user selection.

This optimal policy now simplifies the discrete case in terms of analysis. Calculations are only required during each discrete time step in order to locate the highest performing user. With that analysis, the controller may allocate the respective workload and calculations will continue for the next time step. Due to this model being discretized, the policy may seem suboptimal upon inspection due to comparison with the continuous model. This is as expected due to our constraints from discretizing our time and workloads. The analysis will show that a discrete model will display suboptimal performances when compared with continuous analysis.

Theorem 5. ***(Optimal controller for multiple users in discrete time)*** *Consider N users with fatigue dynamics*

$$x_i(t_{k+1}) = \alpha_i^d x_i(t_k) + b_d u_i(t_k),\ i \in \{1, \dots, N\},$$

where $\alpha_i^d \in \mathbb{R}$, and $x_i(0) = 0$. The task allocation $u_i^* : \mathbb{R} \to [0, 1]$, with $\sum_{i=1}^{N} u_i(t) = 1$ at all times t, that maximizes the cost function

$$J_{D\text{-}M} = \frac{1}{NM} \sum_{i=1}^{N} \sum_{k=1}^{M} P_i^d(t_k) u_i(t_k) T,$$

is as follows:

$$u_i^*(t) = \begin{cases} 1, & \text{if } P_i^d = \max\{P_1^d, \dots, P_N^d\}, \\ 0, & \text{otherwise.} \end{cases}$$

We provide the following simulations to illustrate the differences between our continuous policy vs. our discrete policy. The policy proposed in Theorem 5 is simulated in Fig. 3.10. It may be observed that the discrete policy will for the most part, act

suboptimally compared with our continuous model. Our continuous model will always select the optimal worker for task allocation. The discrete model proposed in the thesis will agree with the continuous model when no users' performance curve intersect in the time frame.

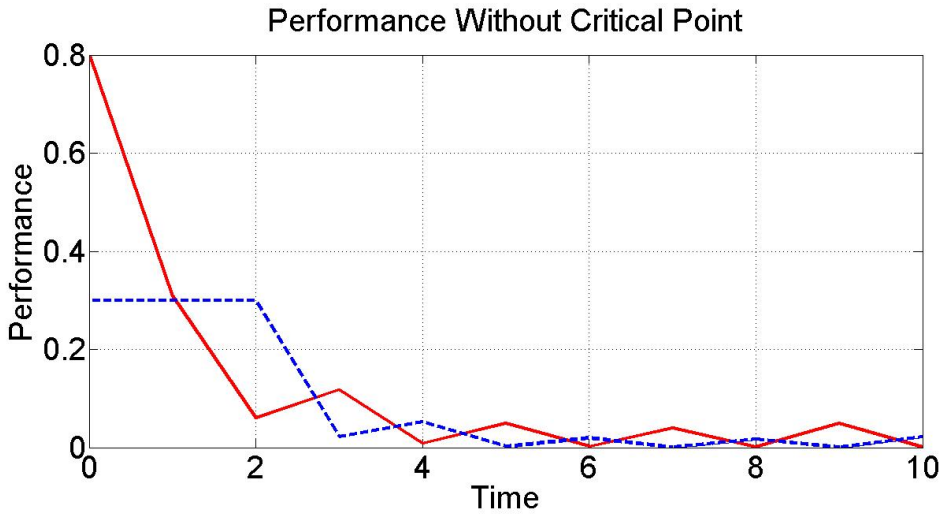

Figure 3.10: This figure illustrates a standard policy where the controller selects the highest performing user at the beginning of each time iteration, and assign him/her with the entire workload.

With the policy given in Theorem 5, we model the performance curves of two arbitrary users in Fig. 3.10. It is noted that each user exhibits a constant performance increase or decrease during each time frame. No user changes workload in the middle of a single time frame, t_k to t_{k+1}. This simulation agrees with our policy assumed in Theorem 5. We compare the overall performance of the discrete policy with our continuous policy. An important note here is our continuous policy was simulated again in a minute scale discretization in order to meet software constraints for our comparison. We also note the slight change in the overall performance for our two continuous simulation due to these software constraints. Calculation time must be considered for the software during simulations. The use of infinitesimal time steps was considered, but the overall performance for the continuous policy would be much higher than the discrete policy.

This substantial difference would make our two models difficult to compare. We provide this comparison as follows in Fig. 3.11.

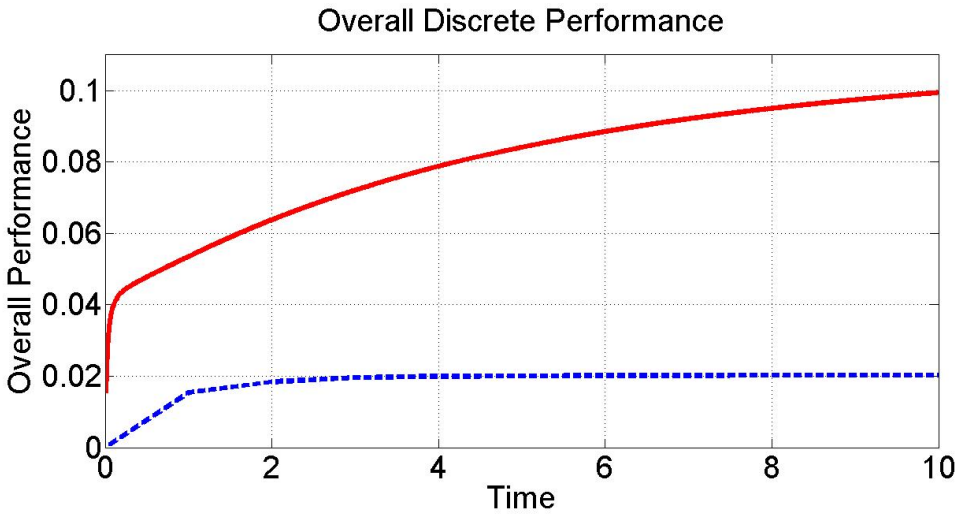

Figure 3.11: In this comparison, we notice a dramatic performance loss due to discretization of the system. This is expected with the mathematical comparisons of our two policies and is in agreement with our conclusion.

Given the comparison shown in Fig. 3.11 above, we conclude that the discrete model's policy has a lower overall performance than the continuous policy as expected. This is due to our discrete time steps inhibiting the controller from selecting a new optimal user. This constraint on the controller forces the controller to select a user who may initially be optimal but acts suboptimally in the long run. This case is very intriguing albeit simplified. The more complicated model considering the integral will be discussed in Chapter 4.2.

Chapter 4

Conclusion and Future Work

Crowdsourcing has the potential to be extremely effective and cost-efficient in modern day task completion. As our society moves towards the "cloud", with the internet being the main medium for conferences, seminars, and task assignments, we begin to unravel the power of crowdsourcing. Communication can be achieved instantaneously with the current state of the internet, allowing crowdsourcing to be possible. Noting the challenges of the emerging method, we offer optimal algorithms for task allocation through crowdsourcing. This thesis focused on designing task allocation algorithms that maximize the performance of users with respect to their fatigue level, recovery rate, and expertise. Our models were hypothesized and validated continually from optimal control theory and dynamical systems. Upon completion of our simulation, we provided visual examples of the data and the performance plot. These figures help convey the success of our task allocation algorithms.

4.1 Summary

In Chapter 2, we presented the basis of our studies and model. We discuss the theory behind each work in current literature that contributed to and motivated our thesis. We provide analytical equations and notation that aided in providing a background for our simulations.

In Chapter 3, we illustrated our model for fatigue and performance, where we validate it with current studies in literature. We extend our method for modeling a user's expertise through the study of the drift diffusion model. We exhibit the variances from these new simulations with our previous examples. Given these dynamic systems, we display our findings through various cases. In particular, we discuss the overall performance of our model considering continuous and discrete time, as well as single and multi-user systems. We conclude the chapter by illustrating our performance curve for each optimal task allocation algorithm.

4.2 Future Work

The studies provided in this thesis discuss simple optimal crowdsourcing algorithms that consider a single exogenous human factor. Despite agreeable performance curves from corresponding algorithms, we must indicate room for future work and improvement. We begin to present elements that must be studied in future research.

In-depth analysis must be completed for complex biological factors that are not fully understood or modeled. Various factors that need to be considered range from boredom, sleep activity, motive, and etc. A large body of findings and studies have been completed in various literature articles [6, 9, 10, 11, 12, 14, 19, 20, 23, 24, 28, 32]. Preliminary studies have been conducted by Vaibhav et al. to implement these complex

models to human robot decision making [31].

Malicious crowd users must also be studied for implementation. In our analysis, we focus on users whose performance is solely based on their fatigue. Assumptions were made that every user will attempt to complete the task with their best efforts. Current studies illustrate that in crowdsourcing, many users provide useless or erroneous answers due to obscurity [16]. New research must implement these bad labels into optimal task allocation algorithms.

Recall from Chapter 3.5 the discussion of our nontrivial integral. A better performing discrete model would consider the integral of our users' performance, $P_i^d(t_k)$. This would be in accordance to our continuous model. The cost function for our discrete model, $J_{\text{D-M}}$, would then be the counterpart to the continuous cost, $J_{\text{C-M}}$, as discussed in Chapter 3.5. The difficulty in this consideration is the approximation of our integral. This model is an important one to consider for future studies.

The last topic for future research considers optimal decision making. Decision making theory must be studied further to accurately model a user's expertise at any point in time. Considering a plethora of factors, inherent and extrinsic, lead to decision making, various studies may be completed to improve the model of a user's expertise. These studies range from network models to prior experience and will help accurately implement the user's expertise into our approximations.

Preliminary studies have been completed to examine a dynamic expertise coefficient that evolves over time. In this thesis, we present early analysis of the drift diffusion model to approximate a dynamic expertise coefficient for our users.

Consider the drift diffusion model following the *interrogation paradigm*. Recall that in the *interrogation paradigm*, the user must select a decision at the end of the time interval based of his/her accumulation of evidence. Let this paradigm be our focus of

analysis. We examine the first pure drift diffusion model from equation (2.4) under the *interrogation paradigm*,

$$dx = Adt + cdW,$$

where we assume the drift A to be 1 and the noise c to be 1. The corresponding performance function is given by

$$P_{\text{interrogation}} = 1 - \Phi\left(-\frac{AT - x_0}{c\sqrt{T}}\right),$$

from equation (2.11), where Φ is the normal cumulative distribution function from equation (2.8), x_0 is the initial condition given by equation (2.10), $A : A \to \mathbb{R}$ is the drift constant, $c : \mathbb{R} \to [0, 1]$ is the noise, and $T \in [0, t_f]$ is the time interval of the model. Let this performance function be our dynamic expertise coefficient,

$$k_i(t) = P_{\text{interrogation}}(t).$$

As expertise increases over time from the drift diffusion model, the performance from equation (3.3) will increase as well. This concurs with our intuition that expertise should improve over time and experience. We model this performance curve with various initial conditions in Fig. 4.1.

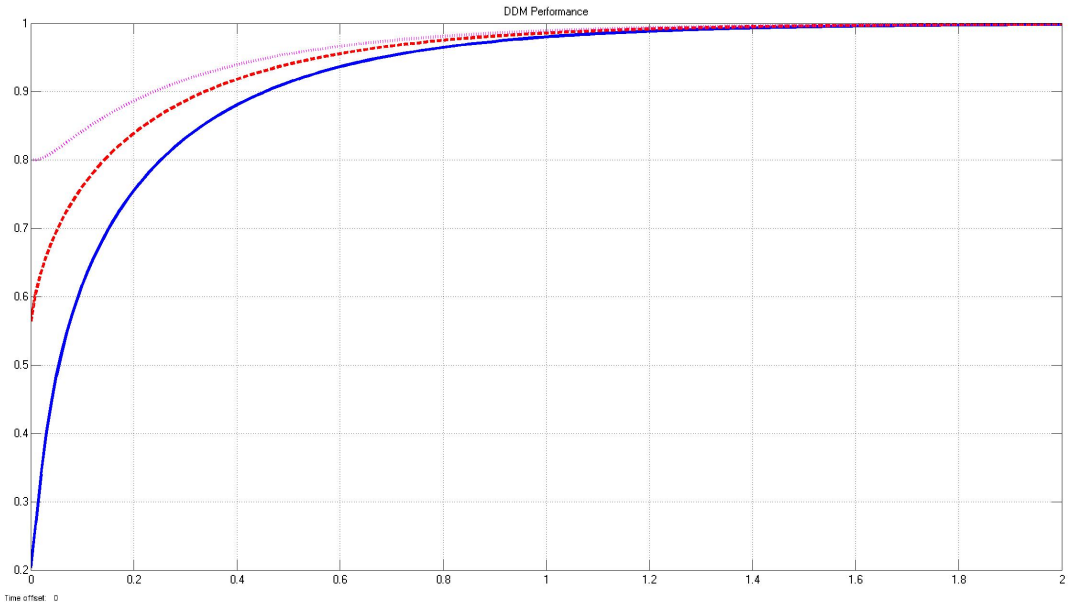

Figure 4.1: This figure represents the simulation of our performance curve from pure drift diffusion in the *interrogation paradigm*.

Now we observe the O-U Model given in equation (2.12), where the users will each learn at a different rate over time. This is opposing the model in Fig. 4.1 where in comparison, each user approaches the same asymptotic learning curve. In the O-U Model, the performance function given by equation (2.14) will have a different evolution with time. Let us examine the equation (2.12) given by,

$$dx = (\lambda x + A)dt + cdW,$$

where $\lambda : \lambda \to \mathbb{R}$ is the reward effect on x as stated in Section 2.1.2. Let the drift $A = 1$, $\lambda = -1 < 0$ to assume a *stable* O-U process, and the noise constant $c = 1$ [2]. Studying the O-U Model where we apply the *interrogation paradigm* provides us with a performance function given by

$$k_i(T) = P_{\text{O-U}}(T) = 1 - \Phi\left(-\frac{A}{c}\sqrt{\frac{2(e^{\lambda T} - 1)}{\lambda(e^{\lambda T} + 1)}}\right),$$

from equation (2.14). We model the performance function above to obtain Fig. 4.2 where we can observe the change of each user's performance over time. This follows the

same intuition that users learn over time, but now we add different limitations to each users' learning curve.

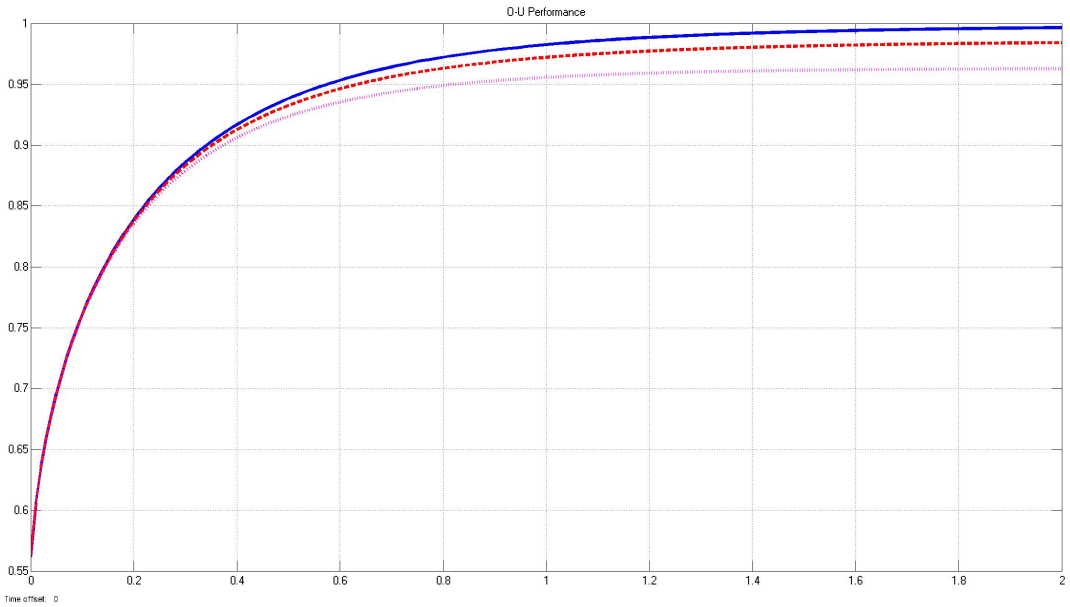

Figure 4.2: This figure represents the simulation of our performance curve for an O-U Model in the *interrogation paradigm*.

Now we present the effects of the drift diffusion model in our optimization models. These simulations are all preliminary studies that form a framework for future research.

The main objective of this thesis is to design task allocation algorithms to maximize the performance of some users, with respect to their fatigue level, recovery rate, and expertise. In the following paragraphs, we detail different scenarios and the corresponding optimal task allocation policies.

The preliminary analyses for evolving the user's expertise coefficient, have been completed and will be shown as follows. We let k_i be dynamic following the drift diffusion model from Section 2.1.2. This thesis presents two models of study for our expertise coefficient: the pure drift diffusion model and the Ornstein-Uhlenbeck (O-U) Model.

Consider the pure drift diffusion model with performance given from equation (2.11),

$$P_{\text{interrogation}} = 1 - \Phi\left(-\frac{AT - x_0}{c\sqrt{T}}\right),$$

where x_0 is the initial condition dependent on π from equation (2.10). Let π range from 0.3 to 0.8 with the equation for x_0 given by

$$x_0 = c^2 \log(\pi/(1-\pi))/2A.$$

Assuming the drift rate $A = 1$, the noise constant $c = 1$, and a time interval $T \in [0, 10]$, we present new simulations with $P_{\text{interrogation}}$ as our k_i. This is displayed in Fig. 4.3 with the corresponding performance shown in Fig. 4.4.

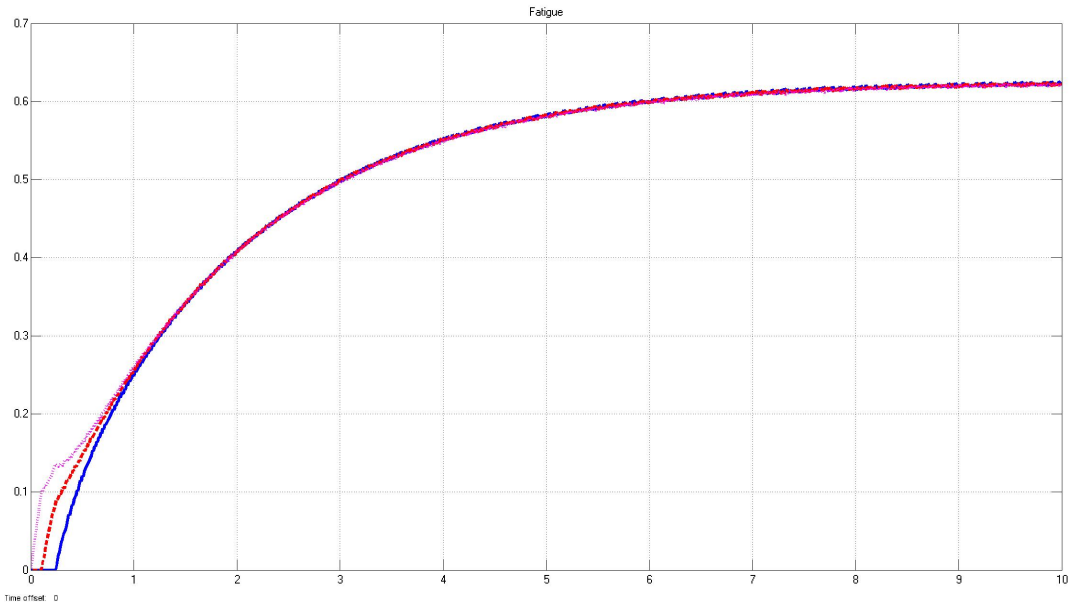

Figure 4.3: This figure shows our fatigue curve from Fig. 3.8(a) with a dynamic expertise coefficient, k_i, based on the drift diffusion model presented in Section 2.1.2.

Comparing Fig. 3.8(b) with Fig. 4.4, we observe a variance early in the curve. Recall that k_i is now modeled as the complement of an error function from equation (2.9). This sigmoidal relationship causes the most variance early in the curve before approaching a saturated value as inspected in Fig. 2.1. This agrees naturally that users will learn over time.

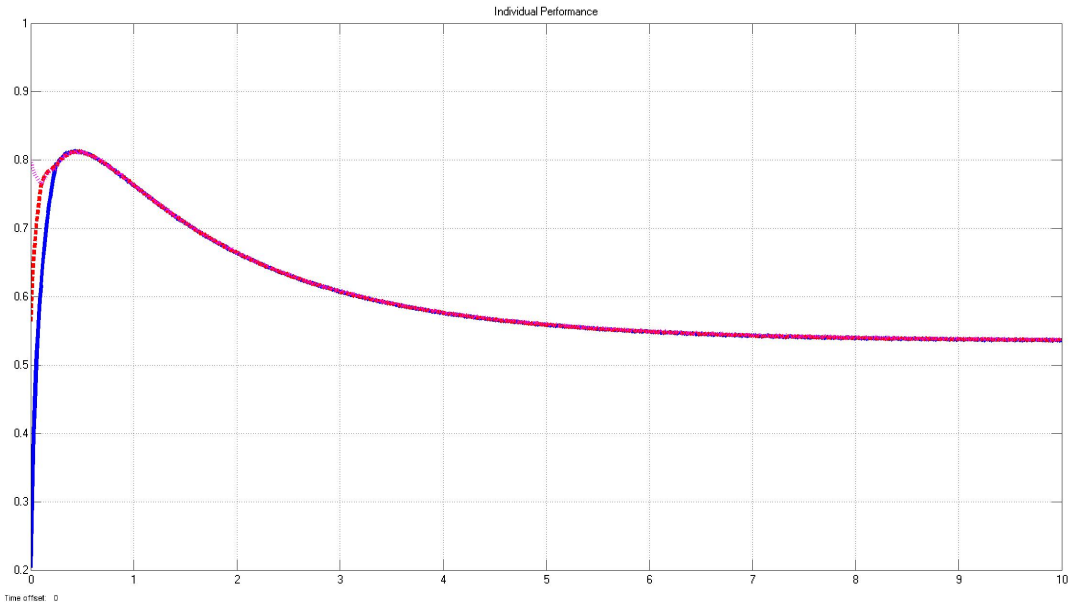

Figure 4.4: This figure shows the plot of our performance obtained from our fatigue model with a dynamic expertise coefficient shown in Fig. 4.3.

Extending our drift diffusion model into the O-U Model, we are presented with a performance function from (2.14),

$$P_{\text{O-U}}(T) = 1 - \Phi\left(-\frac{A}{c}\sqrt{\frac{2(e^{\lambda T}-1)}{\lambda(e^{\lambda T}+1)}}\right),$$

where $\lambda \in \mathbb{R}$ is the leak or reward rate and Φ is a normal cumulative distribution function. Examining Fig. 4.2, we note that in the O-U Model, each user learns at a different rate depending on the value of λ. In comparison, we note that each user reaches the same learning rate in the pure drift diffusion model as inspected from Fig. 4.1. Consider the same parameters from the pure drift diffusion model. We simulate the performance function as our expertise, k_i, to obtain the following:

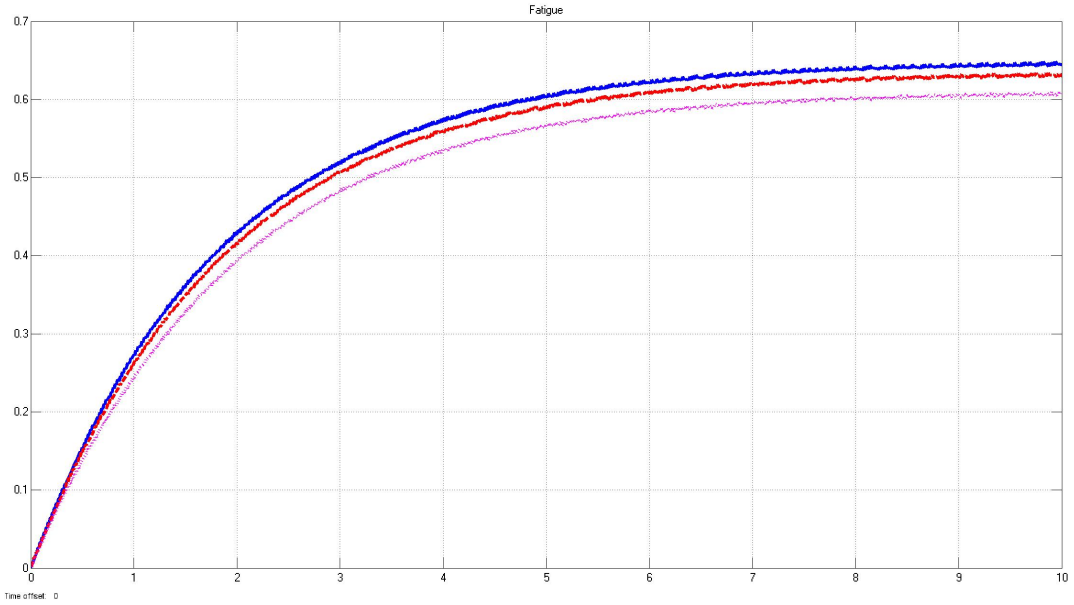

Figure 4.5: The fatigue curve under the O-U drift diffusion model. The fatigue follows equation (3.2).

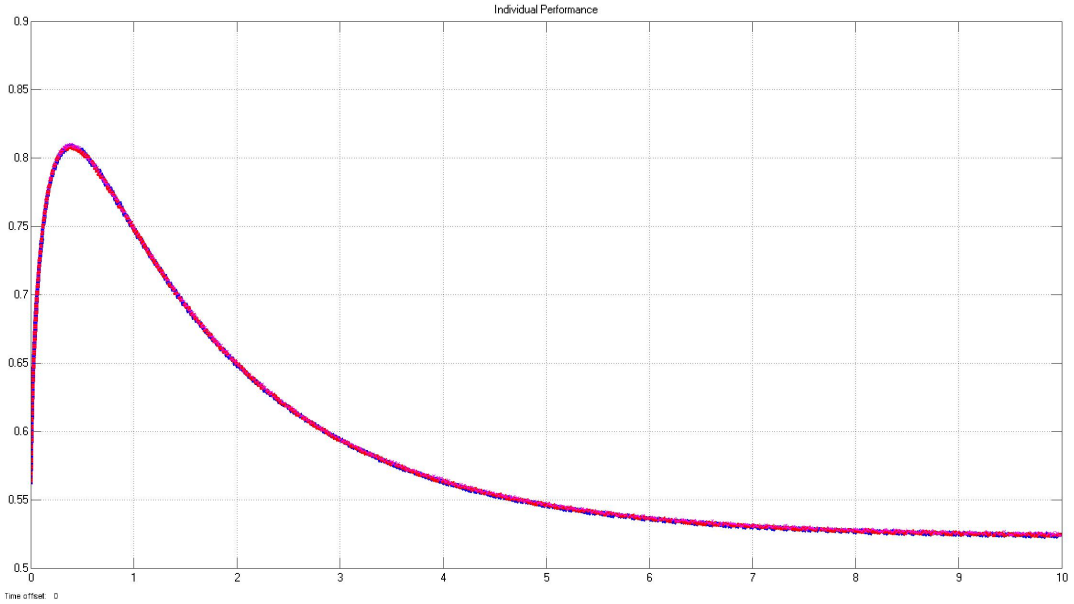

Figure 4.6: Using the performance model from O-U in equation (2.14) in combination with our normal performance model from equation (3.3), we obtain the simulation presented in this figure.

In comparison of Fig. 4.5 and 4.6 above and Fig. 4.3 and 4.4 from earlier, we detect diminutive variances in the general curve. The low initial performance is due to users starting at an extremely low initial expertise. After an interval of time, the fatigue

takes over the performance model as the expertise saturates. These two drift diffusion models become comparable after that time frame.

This study for the expertise evolution becomes a base for future work. Detailed studies for a dynamic expertise coefficient must be completed for a more accurate approximation and analysis of our optimization models.

In conclusion, our studies draw from many different fields in order to assess our problem statement. Each field provides mechanisms that could be studied in depth and improved for future implementation. With our current assumptions, it is seen that our task allocation algorithm is optimal.

Bibliography

[1] M. Athans and P.L. Falb. *Optimal Control: An Introduction to the Theory and Its Applications*. Dover Books on Engineering Series. Dover Publications, 2006.

[2] Rafal Bogacz, Eric Brown, Jeff Moehlis, Philip Holmes, and Jonathan D. Cohen. The physics of optimal decision making: A formal analysis of models of performance in two-alternative forced-choice tasks. *Psychological Review*, 113(4):700–765, 2006.

[3] J. R. Busemeyer and J. T. Townsend. Fundamental derivations from decision field theory. 23:255–282, 1992.

[4] J. R. Busemeyer and J. T. Townsend. Decision field theory: A dynamic-cognitive approach to decision making in an uncertain environment. 100:432–459, 1993.

[5] Andrea Calogero. Notes on optimal control theory, 2014.

[6] Derk-Jan Dijk and Charles A Czeisler. Contribution of the circadian pacemaker and the sleep homeostat to sleep propensity, sleep structure, electroencephalographic slow waves, and sleep spindle activity in humans. *The Journal of neuroscience*, 15(5):3526–3538, 1995.

[7] P. Eckoff, P. Holmes, C. Law, P. M. Connolly, and J. I. Gold. On diffusion processes with variable drift rates as models for decision making during learning. 10, 2008.

[8] G. M. Ewing. *Calculus of Variations with Applications*. Dover, 1985.

[9] S Folkard and T Akerstedt. Towards a model for the prediction of alertness and/or fatigue on different sleep/wake schedules. *Contemporary Advances in Shiftwork Research: Theoretical and Practical Aspects in the Late Eighties. Krakow, Poland: Medical Academy*, pages 231–40, 1987.

[10] Simon Folkard, Rutger A Wever, and Christina M Wildgruber. Multi-oscillatory control of circadian rhythms in human performance. *Nature*, 305(5931):223–226, 1983.

[11] JE Fröberg. Twenty-four-hour patterns in human performance, subjective and physiological variables and differences between morning and evening active subjects. *Biol Psychol*, 5(2), 1977.

[12] Steven R. Hursh, Daniel P. Redmond, Michael L. Johnson, David R. Thorne, Gregory Belenky, Thomas J. Balkin, William F. Storm, James C. Miller, and Douglas R. Eddy. Fatigue models for applied research in warfighting. *Aviation, Space, and Environmental Medicine*, 75(3), 2004.

[13] Eugene Isaacson. *Analysis of numerical methods*. Courier Dover Publications, 1994.

[14] Megan E. Jewett and Richard E. Kronauer. Interactive mathematical models of subjective alertness and cognitive throughput in humans. *Journal of Biological Rhythms*, 14(6):588–597, 1999.

[15] Donald E. Kirk. *Optimal Control Theory, An Introduction*. Dover, 2004.

[16] Qiang Liu, Jian Peng, and Alexander Ihler. Variational inference for crowdsourcing. pages 701–709, 2012.

[17] James M. Longuski, Jose J. Guzman, and John E. Prussing. The minimum principle. In *Optimal Control with Aerospace Applications*, volume 32 of *Space Technology Library*, pages 105–129. Springer New York, 2014.

[18] James M. Longuski, Jose J. Guzman, and John E. Prussing. The weierstrass condition. In *Optimal Control with Aerospace Applications*, volume 32 of *Space Technology Library*, pages 95–103. Springer New York, 2014.

[19] Melissa M. Mallis, Sig Mejdal, Tammy T. Nguyen, and David F. Dinges. Summary of the key features of seven biomathematical models of human fatigue and performance. *Aviation, Space, and Environmental Medicine*, 75(3):A4–A14, 2004.

[20] T. H. Monk and D. E. Embrey. A field study of circadian rhythms in actual and interpolated task performance. *Night and shift work: Biological and social aspects*, pages 473–480, 1981.

[21] J. Neyman and E. S. Pearson. On the problem of the most efficient tests of statistical hypothesis. 231:289–337, 1933.

[22] N.D. Powel and K.A. Morgansen. Multiserver queueing for supervisory control of autonomous vehicles. pages 3179–3185, 2012.

[23] Torbjörn Åkerstedt and Simon Folkard. The three-process model of alertness and its extension to performance, sleep latency, and sleep length. *Chronobiology International*, 14(2):115–123, 1997. PMID: 9095372.

[24] Torbjörn Åkerstedt, Simon Folkard, and Christian Portin. Predictions from the three-process model of alertness. *Aviation, Space, and Environmental Medicine*, 75(3):A75–A83, 2004.

[25] Roger Ratcliff. A theory of memory retrieval. *Psychological Review*, 85(2):59–108, 1978.

[26] Roger Ratcliff and Gail McKoon. The diffusion decision model: Theory and data for two-choice decision tasks. *Neural Computation*, 20(4):873 – 922, 2008.

[27] Roger Ratcliff and Philip L. Smith. A comparison of sequential sampling models for two-choice reaction time. 111(2):333–367, 2004.

[28] Robert L. Sack, Dennis Auckley, Robert R. Auger, Mary A. Carskadon, Kenneth P. Wright Jr., Michael V. Vitiello, and Irina V. Zhdanova. Circadian rhythm sleep disorders: Part i, basic principles, shift work and jet lag disorders. an american academy of sleep medicine review. *Sleep*, 30(11):1460–1483, 2007.

[29] Vicki Sealey. Definite integrals, riemann sums, and area under a curve: What is necessary and sufficient. In *Proceedings of the 28th Annual Meeting of the North American Chapter of the International Group for the Psychology of Mathematics Education*, volume 2, page 46. Universidad Pedagogica Nacional Merida, Mexico, 2006.

[30] V. Srivastava and N. E. Leonard. On the speed-accuracy trade-off in collective decision making. *IEEE Conf. on Decision and Control*, pages 1880–1885, 2013.

[31] Vaibhav Srivastava, Amit Surana, Miguel P. Eckstein, and Francesco Bullo. Mixed human-robot team surveillance. *arXiv preprint*, 2013.

[32] R. Wever. Mathematical models of circadian one- and multi-oscillator systems. *Some Mathematical Question in Biology: Circadian Rhythms*, 18:205, 1987.

[33] Laurence Young. *Lecture on the Calculus of Variations and Optimal Control Theory.* American Mathematical Society, 1980.